

1 **Mitochondrial respiratory states and rates:**
2 **Building blocks of mitochondrial physiology Part 1**
3

4 **MitoEAGLE preprint** Version: 2018-03-20(34)

5 Corresponding author: Gnaiger E

6 Co-authors:

7 Aasander Frostner E, Abumrad NA, Acuna-Castroviejo D, Ahn B, Ali SS, Alves MG, Amati
8 F, Aral C, Arandarčikaitė O, Bailey DM, Bajpeyi S, Bakker BM, Bastos Sant'Anna Silva AC,
9 Battino M, Bazil J, Beard DA, Bednarczyk P, Ben-Shachar D, Bergdahl A, Bernardi P,
10 Bishop D, Blier PU, Boetker HE, Boros M, Borsheim E, Borutaitė V, Bouillaud F, Bouitbir J,
11 Breton S, Brown DA, Brown GC, Brown RA, Buettner GR, Burtscher J, Calabria E, Calbet
12 JA, Calzia E, Cannon DT, Canto AC, Cardoso LHD, Carvalho E, Casado Pinna M,
13 Cavalcanti-de-Albuquerque JP, Cervinkova Z, Chang SC, Chaurasia B, Chen Q, Chicco AJ,
14 Chinopoulos C, Clementi E, Coen PM, Coker RH, Collin A, Crisóstomo L, Das AM, Dash
15 RK, Davis MS, De Palma C, Dembinska-Kiec A, Dias TR, Distefano G, Doerrier C, Drahota
16 Z, Dubouchaud H, Duchen MR, Dumas JF, Durham WJ, Dymkowska D, Dyrstad SE,
17 Dzialowski EM, Ehinger J, Elmer E, Endlicher R, Engin AB, Fell DA, Ferko M, Ferreira
18 JCB, Ferreira R, Fessel JP, Filipovska A, Fisar Z, Fischer M, Fisher G, Fisher JJ, Fornaro M,
19 Galkin A, Gan Z, Garcia-Roves PM, Garcia-Souza LF, Garlid KD, Garrabou G, Garten A,
20 Gastaldelli A, Genova ML, Giovarelli M, Gonzalez-Armenta JL, Gonzalo H, Goodpaster BH,
21 Gorr TA, Gourlay CW, Granata C, Grefte S, Haas CB, Haavik J, Haendeler J, Han J, Hancock
22 CR, Hand SC, Hargreaves I, Harrison DK, Hellgren KT, Hepple RT, Hernansanz-Agustin P,
23 Hickey AJ, Hoel F, Holland OJ, Holloway GP, Hoppel CL, Houstek J, Hunger M, Iglesias-
24 Gonzalez J, Irving BA, Iyer S, Jackson CB, Jadiya P, Jang DH, Jang YC, Jansen-Dürr P,
25 Jespersen NR, Jha RK, Jurk D, Kaambre T, Kainulainen H, Kane DA, Kappler L,
26 Karabatsiakakis A, Keijer J, Keppner G, Khamoui AV, Klingenspor M, Komlodi T, Koopman
27 WJH, Kopitar-Jerala N, Kowaltowski AJ, Krajcova A, Krako Jakovljevic N, Kuang J, Kucera
28 O, Kwak HB, Kwast K, Labieniec-Watala M, Lai N, Land JM, Lane N, Laner V, Lanza IR,
29 Larsen TS, Lavery GG, Lee HK, Leeuwenburgh C, Lemieux H, Lerfall J, Li PA, Liu J,
30 Lucchinetti E, Macedo MP, MacMillan-Crow LA, Makrecka-Kuka M, Malik A, Markova M,
31 Martin DS, Mazat JP, McKenna HT, Menze MA, Meszaros AT, Methner A, Michalak S,
32 Moiso N, Molina AJA, Montaigne D, Moreau K, Moore AL, Moreira BP, Mracek T,
33 Muntane J, Muntean DM, Murray AJ, Nair KS, Nemeč M, Neuffer PD, Neuzil J, Newsom S,
34 Nozickova K, O'Gorman D, Oliveira MF, Oliveira MT, Oliveira PF, Oliveira PJ, Orynbayeva
35 Z, Osiewacz HD, Pak YK, Pallotta ML, Palmeira CM, Parajuli N, Passos JF, Patel HH,
36 Pecina P, Pelnena D, Pereira da Silva Grilo da Silva F, Pesta D, Petit PX, Pettersen IKN,
37 Pichaud N, Piel S, Pietka TA, Pino MF, Pirkmajer S, Porter C, Porter RK, Pranger F,
38 Prochownik EV, Pulinilkunnit T, Puskarich MA, Puurand M, Radenkovic F, Radi R, Ramzan
39 R, Rattan S, Reboredo P, Renner-Sattler K, Robinson MM, Roden M, Rohlena J, Rolo AP,
40 Ropelle ER, Røslund GV, Rossiter HB, Rybacka-Mossakowska J, Saada A, Safaei Z, Salin K,
41 Salvadego D, Sandi C, Sazanov LA, Scatena R, Schartner M, Scheibye-Knudsen M, Schilling
42 JM, Schlattner U, Schönfeld P, Schwarzer C, Scott GR, Shabalina IG, Sharma P, Sharma V,
43 Shevchuk I, Siewiera K, Silber AM, Silva AM, Sims CA, Singer D, Skolik R, Smenes BT,
44 Smith J, Soares FAA, Sobotka O, Sokolova I, Sonkar VK, Sparks LM, Spinazzi M, Stankova
45 P, Stary C, Stier A, Stocker R, Sumbalova Z, Suravajhala P, Swerdlow RH, Swiniuch D,
46 Tanaka M, Tandler B, Tavernarakis N, Tepp K, Thyfault JP, Tomar D, Towheed A, Tretter L,
47 Trifunovic A, Trivigno C, Tronstad KJ, Trougakos IP, Tyrrell DJ, Urban T, Valentine JM,
48 Velika B, Vendelin M, Vercesi AE, Victor VM, Vieyra A Villena JA, Vitorino RMP, Vogt S,
49 Volani C, Votion DM, Vujacic-Mirski K, Wagner BA, Ward ML, Wasserman DH, Watala C,
50 Wei YH, Wieckowski MR, Williams C, Wohlgemuth SE, Wohlwend M, Wolff J, Wüst RCI,
51 Yokota T, Zablocki K, Zaugg K, Zaugg M, Zhang Y, Zischka H, Zorzano A

Updates and discussion:

http://www.mitoeagle.org/index.php/MitoEAGLE_preprint_2018-02-08

Correspondence: Gnaiger E

Chair COST Action CA15203 MitoEAGLE – <http://www.mitoeagle.org>

*Department of Visceral, Transplant and Thoracic Surgery, D. Swarovski Research
Laboratory, Medical University of Innsbruck, Innrain 66/4, A-6020 Innsbruck, Austria*

Email: mitoeagle@i-med.ac.at

Tel: +43 512 566796, Fax: +43 512 566796 20

Contents**Abstract****Executive summary****1. Introduction** – Box 1: In brief: Mitochondria and Bioblasts**2. Oxidative phosphorylation and coupling states in mitochondrial preparations**

Mitochondrial preparations

2.1. Respiratory control and coupling

The steady-state

Specification of biochemical dose

Phosphorylation, P_{\gg} , and P_{\gg}/O_2 ratio

Control and regulation

Respiratory control and response

Respiratory coupling control and ET-pathway control

Coupling

Uncoupling

2.2. Coupling states and respiratory rates

Respiratory capacities in coupling control states

LEAK, OXPHOS, ET, ROX

Quantitative relations

2.3. Classical terminology for isolated mitochondria

States 1–5

3. Normalization: fluxes and flows*3.1. Normalization: system or sample*

Flow per system, I

Extensive quantities

Size-specific quantities – Box 2: Metabolic fluxes and flows: vectorial and scalar

3.2. Normalization for system-size: flux per chamber volume

System-specific flux, J_{V,O_2}

3.3. Normalization: per sample

Sample concentration, C_{mX}

Mass-specific flux, $J_{O_2/mX}$

Number concentration, C_{NX}

Flow per object, $I_{O_2/X}$

3.4. Normalization for mitochondrial content

Mitochondrial concentration, C_{mtE} , and mitochondrial markers

Mitochondria-specific flux, $J_{O_2/mtE}$

*3.5. Evaluation of mitochondrial markers**3.6. Conversion: units***4. Conclusions****5. References**

103 **Abstract** As the knowledge base and importance of mitochondrial physiology to human health
104 expands, the necessity for harmonizing nomenclature concerning mitochondrial respiratory
105 states and rates has become increasingly apparent. Clarity of concept and consistency of
106 nomenclature are key trademarks of a research field. These features facilitate effective
107 transdisciplinary communication, education, and ultimately further discovery. The
108 chemiosmotic theory establishes the mechanism of energy transformation and coupling in
109 oxidative phosphorylation. The unifying concept of the protonmotive force provides the
110 framework for developing a consistent theoretical foundation of mitochondrial physiology and
111 bioenergetics. We follow IUPAC guidelines on terminology in physical chemistry, extended
112 by considerations on open systems and irreversible thermodynamics. The concept-driven
113 constructive terminology incorporates the meaning of each quantity and aligns concepts and
114 symbols to the nomenclature of classical bioenergetics. In the frame of COST Action
115 MitoEAGLE open to global bottom-up input, we endeavour to provide a balanced view on
116 mitochondrial respiratory control and a critical discussion on reporting data of mitochondrial
117 respiration in terms of metabolic flows and fluxes. Uniform standards for evaluation of
118 respiratory states and rates will ultimately support the development of databases of
119 mitochondrial respiratory function in species, tissues, and cells.

120

121 *Keywords:* Mitochondrial respiratory control, coupling control, mitochondrial
122 preparations, protonmotive force, uncoupling, oxidative phosphorylation, OXPHOS,
123 efficiency, electron transfer, ET; proton leak, LEAK, residual oxygen consumption, ROX, State
124 2, State 3, State 4, normalization, flow, flux, O₂

125

126 **Executive summary**

127

- 128 1. In view of the broad implications for health care, mitochondrial researchers face an
129 increasing responsibility to disseminate their fundamental knowledge and novel
130 discoveries to a wide range of stakeholders and scientists beyond the group of
131 specialists. This requires implementation of a commonly accepted terminology
132 within the discipline and standardization in the translational context. Authors,
133 reviewers, journal editors, and lecturers are challenged to collaborate with the aim
134 to harmonize the nomenclature in the growing field of mitochondrial physiology
135 and bioenergetics.
- 136 2. Aerobic respiration depends on the coupling of phosphorylation (ADP → ATP) to O₂
137 flux in catabolic reactions. Coupling in oxidative phosphorylation is mediated by
138 translocation of protons across the inner mitochondrial membrane through proton
139 pumps generating or utilizing the protonmotive force, measured between the
140 mitochondrial matrix and intermembrane compartment. Compartmental coupling
141 distinguishes vectorial oxidative phosphorylation from glycolytic fermentation as
142 the counterpart of cellular core energy metabolism (**Figure 1**).
- 143 3. To exclude fermentation and other cytosolic interactions from exerting an effect on the
144 analysis of mitochondrial metabolism, the barrier function of the plasma membrane
145 must be disrupted. Selective removal or permeabilization of the plasma membrane
146 yields mitochondrial preparations—including isolated mitochondria, tissue and
147 cellular preparations—with structural and functional integrity. Then extra-
148 mitochondrial concentrations of fuel substrates, ADP, ATP, inorganic phosphate,
149 and cations including H⁺ can be controlled to determine mitochondrial function
150 under a set of conditions defined as coupling control states. A concept-driven
151 terminology of bioenergetics explicitly incorporates in its terms and symbols
152 information on the nature of respiratory states that makes the technical terms readily
153 recognized and more easy to understand.

154 **Figure 1. Mitochondrial respiration is the**
 155 **oxidation of fuel substrates and reduction of**
 156 **O₂ catalysed by the electron transfer system,**
 157 **ETS: (a) catabolic respiration (including non-**
 158 **mitochondrial oxidation reactions, b), and**
 159 **oxygen balance of internal (c) and external (d)**
 160 **respiration**

161 All chemical reactions, r , that consume O₂ in the
 162 cells of an organism, contribute to cell
 163 respiration, J_{rO_2} . ❶ Non-mitochondrial O₂
 164 consumption by catabolic reactions, particularly
 165 peroxisomal oxidases; ❷ mitochondrial residual
 166 oxygen consumption, R_{ox} , after blocking the
 167 ETS; ❸ non-mitochondrial R_{ox} ; ❹ extracellular
 168 O₂ consumption; ❺ aerobic microbial respiration.
 169 Bars are not at a quantitative scale.

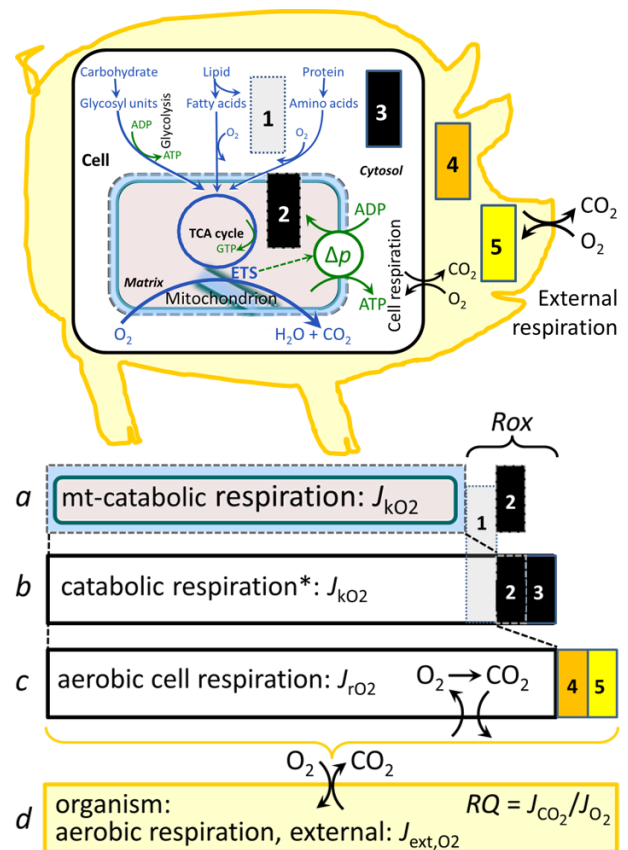
170 **a Mitochondrial catabolic respiration, J_{kO_2} ,** is
 171 the O₂ consumption by the mitochondrial ETS
 172 maintaining the protonmotive force, Δp . J_{kO_2}
 173 excludes R_{ox} .

174 **b Catabolic respiration** is the O₂ consumption
 175 associated with catabolic pathways in the cell,
 176 including peroxisomal oxidation reactions (❶)
 177 in addition to mitochondrial catabolism (* The
 178 reactions k have to be defined specifically for a and b .)

179 **c Aerobic cell respiration, J_{rO_2} ,** takes into account internal O₂-consuming reactions, r ,
 180 including catabolic respiration and R_{ox} . Internal respiration of an organism includes
 181 extracellular O₂ consumption (❹) and aerobic respiration by the microbiome (❺).
 182 Respiration is distinguished from fermentation by: (1) External electron acceptors for the
 183 maintenance of redox balance, whereas fermentation is characterized by an internal electron
 184 acceptor produced in intermediary metabolism. In aerobic cell respiration, redox balance is
 185 maintained by O₂ as the electron acceptor. (2) Compartmental coupling in vectorial oxidative
 186 phosphorylation, in contrast to exclusively scalar substrate-level phosphorylation in
 187 fermentation.

188 **d External respiration** balances internal respiration at steady-state. O₂ is transported from the
 189 environment across the respiratory cascade (circulation between tissues and diffusion across
 190 cell membranes) to the intracellular compartment, while bicarbonate and CO₂ are transported
 191 in reverse to the extracellular milieu and the organismic environment. Hemoglobin provides
 192 the molecular paradigm for the combination of O₂ and CO₂ exchange, as do lungs and gills
 193 on the morphological level. The respiratory quotient, RQ , is the molar CO₂/O₂ exchange
 194 ratio; when combined with the respiratory nitrogen quotient, N/O₂ (mol N given off per mol
 195 O₂ consumed), the RQ reflects the proportion of carbohydrate, lipid and protein utilized in
 196 cell respiration during aerobically balanced steady-states.

197
 198 4. Mitochondrial coupling states are defined according to the control of respiratory oxygen
 199 flux by the protonmotive force. Capacities of oxidative phosphorylation and
 200 electron transfer are measured at kinetically saturating concentrations of fuel
 201 substrates, ADP and inorganic phosphate, or at optimal uncoupler concentrations,
 202 respectively. Respiratory capacity is a measure of the upper bound of the rate of
 203 respiration, depends on the substrate type undergoing oxidation, and provides
 204 reference values for the diagnosis of health and disease, and for evaluation of the



- 205 effects of Evolutionary background, Age, Gender and sex, Lifestyle and
 206 Environment (EAGLE).
- 207 5. Incomplete tightness of coupling, *i.e.*, some degree of uncoupling relative to the
 208 substrate-dependent coupling stoichiometry, is a characteristic of energy-
 209 transformations across membranes. Uncoupling is caused by a variety of
 210 physiological, pathological, toxicological, pharmacological and environmental
 211 conditions that exert an influence not only on the proton leak and cation cycling,
 212 but also on proton slip within the proton pumps and the structural integrity of the
 213 mitochondria. A more loosely coupled state is induced by stimulation of
 214 mitochondrial superoxide formation and the bypass of proton pumps. In addition,
 215 uncoupling by application of protonophores represents an experimental
 216 intervention for the transition from a well-coupled to the noncoupled state of
 217 mitochondrial respiration.
- 218 6. Respiratory oxygen consumption rates have to be carefully normalized to enable meta-
 219 analytic studies beyond the specific question of a particular experiment. Therefore,
 220 all raw data should be published in a supplemental table or open access data
 221 repository. Normalization of rates for the volume of the experimental chamber (the
 222 measuring system) is distinguished from normalization for: (1) the volume or mass
 223 of the experimental sample; (2) the number of objects (cells, organisms); and (3)
 224 the concentration of mitochondrial markers in the chamber.
- 225 7. The consistent use of terms and symbols will facilitate transdisciplinary communication
 226 and support further developments of a database on bioenergetics and mitochondrial
 227 physiology. The present considerations are focused on studies with mitochondrial
 228 preparations. These will be extended in a series of reports on pathway control of
 229 mitochondrial respiration, the protonmotive force, respiratory states in intact cells,
 230 and harmonization of experimental procedures.
 231

232
 233
 234

235 **Box 1: In brief – Mitochondria and Bioblasts**

236 *‘For the physiologist, mitochondria afforded the first opportunity for an*
 237 *experimental approach to structure-function relationships, in particular those*
 238 *involved in active transport, vectorial metabolism, and metabolic control*
 239 *mechanisms on a subcellular level’ (Ernster and Schatz 1981).*

240 **Mitochondria** are the oxygen-consuming electrochemical generators evolved from
 241 endosymbiotic bacteria (Margulis 1970; Lane 2005). They were described by Richard Altmann
 242 (1894) as ‘bioblasts’, which include not only the mitochondria as presently defined, but also
 243 symbiotic and free-living bacteria. The word ‘mitochondria’ (Greek mitos: thread; chondros:
 244 granule) was introduced by Carl Benda (1898).

245 Mitochondria are dynamic networks contained within eukaryotic cells morphologically
 246 characterized by a double membrane. The mitochondrial inner membrane (mtIM) shows
 247 dynamic tubular to disk-shaped cristae that separate the mitochondrial matrix, *i.e.*, the
 248 negatively charged internal mitochondrial compartment, from the intermembrane space; the
 249 latter being positively charged and enclosed by the mitochondrial outer membrane (mtOM).
 250 The mtIM contains the non-bilayer phospholipid cardiolipin, which is not present in any other
 251 eukaryotic cellular membrane. Cardiolipin promotes the formation of respiratory
 252 supercomplexes (SC I_nIII_nIV_n), which are supramolecular assemblies based upon specific,
 253 though dynamic interactions between individual respiratory complexes (Greggio *et al.* 2017;
 254 Lenaz *et al.* 2017). Membrane fluidity exerts an influence on functional properties of proteins
 255 incorporated in the membranes (Waczulikova *et al.* 2007). In addition to mitochondrial
 256 movement along microtubules, mitochondrial morphology can change in response to energy

257 requirements of the cell via processes known as fusion and fission, through which mitochondria
258 communicate within a network, and in response to intracellular stress factors causing swelling
259 and ultimately permeability transition.

260 Mitochondria are the structural and functional elements of cell respiration. Mitochondrial
261 respiration is the reduction of oxygen by electron transfer coupled to electrochemical proton
262 translocation across the mtIM. In the process of oxidative phosphorylation (OXPHOS), the
263 catabolic reaction of oxygen consumption is electrochemically coupled to the transformation of
264 energy in the form of adenosine triphosphate (ATP; Mitchell 1961, 2011). Mitochondria are the
265 powerhouses of the cell which contain the machinery of the OXPHOS-pathways, including
266 transmembrane respiratory complexes (proton pumps with FMN, Fe-S and cytochrome *b*, *c*,
267 *aa*₃ redox systems); alternative dehydrogenases and oxidases; the coenzyme ubiquinone (Q);
268 F-ATPase or ATP synthase; the enzymes of the tricarboxylic acid cycle, fatty acid and
269 aminoacid oxidation; transporters of ions, metabolites and co-factors; and mitochondrial
270 kinases related to energy transfer pathways. The mitochondrial proteome comprises over 1,200
271 proteins (Calvo *et al.* 2015; 2017), mostly encoded by nuclear DNA (nDNA), with a variety of
272 functions, many of which are relatively well known (*e.g.*, proteins regulating mitochondrial
273 biogenesis or apoptosis), while others are still under investigation, or need to be identified (*e.g.*,
274 alanine transporter). Only lately it is possible to use the mammalian mitochondrial proteome to
275 discover and characterize the genetic basis of mitochondrial diseases (Williams *et al.* 2016;
276 Palmfeldt and Bross 2017).

277 There is a constant crosstalk between mitochondria and the other cellular components.
278 The crosstalk between mitochondria and endoplasmic reticulum is involved in the regulation of
279 calcium homeostasis, cell division, autophagy, differentiation, and anti-viral signaling (Murley
280 and Nunnari 2016). Mitochondria contribute to the formation of peroxisomes, which are hybrids
281 of mitochondrial and ER-derived precursors (Sugiura *et al.* 2017). Cellular mitochondrial
282 homeostasis (mitostasis) is maintained through regulation at both the transcriptional and post-
283 translational level. Cell signalling modules contribute to homeostatic regulation throughout the
284 cell cycle or even cell death by activating proteostatic modules (*e.g.*, the ubiquitin-proteasome
285 and autophagy-lysosome pathways) and genome stability modules in response to varying
286 energy demands and stress cues (Quiros *et al.* 2016). Mitochondria can traverse cell boundaries
287 in a process known as horizontal mitochondrial transfer between cells (Torralba *et al.* 2016).

288 Mitochondria typically maintain several copies of their own circular genome known as
289 mitochondrial DNA (mtDNA; hundred to thousands per cell; Cummins 1998), which is
290 maternally inherited. Biparental mitochondrial inheritance is documented in mammals, birds,
291 fish, reptiles and invertebrate groups, and is even the norm in bivalves (Breton *et al.* 2007;
292 White *et al.* 2008). mtDNA is compact (16.5 kB in humans) and encodes 13 protein subunits
293 of the transmembrane respiratory Complexes CI, CIII, CIV and F-ATPase, 22 tRNAs, and two
294 RNAs. Additional gene content has been suggested to include microRNAs, piRNA,
295 smithRNAs, repeat associated RNA, and even additional proteins (Duarte *et al.* 2014; Lee *et al.*
296 *et al.* 2015; Cobb *et al.* 2016). The mitochondrial genome requires nuclear-encoded
297 mitochondrially targeted proteins for its maintenance and expression (Rackham *et al.* 2012).

298 Mitochondrial dysfunction is associated with a wide variety of genetic and degenerative
299 diseases. Robust mitochondrial function is supported by physical exercise and caloric balance,
300 and is central for sustained metabolic health throughout life. Therefore, a more consistent
301 presentation of mitochondrial physiology will improve our understanding of the etiology of
302 disease, the diagnostic repertoire of mitochondrial medicine, with a focus on protective
303 medicine, lifestyle and healthy aging.

304 Abbreviation: mt, as generally used in mtDNA. Mitochondrion is singular and
305 mitochondria is plural.

306
307

308 1. Introduction

309

310 Mitochondria are the powerhouses of the cell with numerous physiological, molecular,
311 and genetic functions (**Box 1**). Every study of mitochondrial health and disease is faced with
312 **E**volution, **A**ge, **G**ender and sex, **L**ifestyle, and **E**nvironment (EAGLE) as essential background
313 conditions intrinsic to the individual patient or subject, cohort, species, tissue and to some extent
314 even cell line. As a large and coordinated group of laboratories and researchers, the mission of
315 the global MitoEAGLE Network is to generate the necessary scale, type, and quality of
316 consistent data sets and conditions to address this intrinsic complexity. Harmonization of
317 experimental protocols and implementation of a quality control and data management system
318 are required to interrelate results gathered across a spectrum of studies and to generate a
319 rigorously monitored database focused on mitochondrial respiratory function. In this way,
320 researchers within the same and across different disciplines can compare findings across
321 traditions and generations to clearly defined and accepted international standards.

322 Reliability and comparability of quantitative results depend on the accuracy of
323 measurements under strictly-defined conditions. A conceptual framework is required to warrant
324 meaningful interpretation and comparability of experimental outcomes carried out by research
325 groups at different institutes. With an emphasis on quality of research, collected data can be
326 useful far beyond the specific question of a particular experiment. Enabling meta-analytic
327 studies is the most economic way of providing robust answers to biological questions (Cooper
328 *et al.* 2009). Vague or ambiguous jargon can lead to confusion and may relegate valuable
329 signals to wasteful noise. For this reason, measured values must be expressed in standard units
330 for each parameter used to define mitochondrial respiratory function. Harmonization of
331 nomenclature and definition of technical terms are essential to improve the awareness of the
332 intricate meaning of current and past scientific vocabulary, for documentation and integration
333 into databases in general, and quantitative modelling in particular (Beard 2005). The focus on
334 coupling states and fluxes through metabolic pathways of aerobic energy transformation in
335 mitochondrial preparations is a first step in the attempt to generate a conceptually-oriented
336 nomenclature in bioenergetics and mitochondrial physiology. Coupling states of intact cells,
337 the protonmotive force, and respiratory control by fuel substrates and specific inhibitors of
338 respiratory enzymes will be reviewed in subsequent communications.

339

340

341 2. Oxidative phosphorylation and coupling states in mitochondrial preparations

342 *‘Every professional group develops its own technical jargon for talking about matters of*
343 *critical concern ... People who know a word can share that idea with other members of*
344 *their group, and a shared vocabulary is part of the glue that holds people together and*
345 *allows them to create a shared culture’ (Miller 1991).*

346

347 **Mitochondrial preparations** are defined as either isolated mitochondria, or tissue and
348 cellular preparations in which the barrier function of the plasma membrane is disrupted. Since
349 this entails the loss of cell viability, mitochondrial preparations are not studied *in vivo*. In
350 contrast to isolated mitochondria and tissue homogenate preparations, mitochondria in
351 permeabilized tissues and cells are *in situ* relative to the plasma membrane. The plasma
352 membrane separates the intracellular compartment including the cytosol, nucleus, and
353 organelles from the environment of the cell. The plasma membrane consists of a lipid bilayer
354 with embedded proteins and attached organic molecules that collectively control the selective
355 permeability of ions, organic molecules, and particles across the cell boundary. The intact
356 plasma membrane prevents the passage of many water-soluble mitochondrial substrates and
357 inorganic ions—such as succinate, adenosine diphosphate (ADP) and inorganic phosphate (P_i),
358 that must be controlled at kinetically-saturating concentrations for the analysis of respiratory

359 capacities; this limits the scope of investigations into mitochondrial respiratory function in
360 intact cells (**Figure 2A**).

361 The cholesterol content of the plasma membrane is high compared to mitochondrial
362 membranes. Therefore, mild detergents—such as digitonin and saponin—can be applied to
363 selectively permeabilize the plasma membrane by interaction with cholesterol and allow free
364 exchange of organic molecules and inorganic ions between the cytosol and the immediate cell
365 environment, while maintaining the integrity and localization of organelles, cytoskeleton, and
366 the nucleus. Application of optimum concentrations of permeabilization agents (mild detergents
367 or toxins) leads to washout of cytosolic marker enzymes—such as lactate dehydrogenase—and
368 results in the complete loss of cell viability, tested by nuclear staining using membrane-
369 impermeable dyes, while mitochondrial function remains intact. Respiration of isolated
370 mitochondria remains unaltered after the addition of low concentrations of digitonin or saponin.
371 In addition to mechanical cell disruption during homogenization of tissue, permeabilization
372 agents may be applied to ensure permeabilization of all cells. Suspensions of cells
373 permeabilized in the respiration chamber and crude tissue homogenates contain all components
374 of the cell at highly dilute concentrations. All mitochondria are retained in chemically-
375 permeabilized mitochondrial preparations and crude tissue homogenates. In the preparation of
376 isolated mitochondria, the cells or tissues are homogenized, and the mitochondria are separated
377 from other cell fractions and purified by differential centrifugation, entailing the loss of a
378 fraction of the total mitochondrial content. Typical mitochondrial recovery ranges from 30% to
379 80%. Maximization of the purity of isolated mitochondria may compromise not only the
380 mitochondrial yield but also the structural and functional integrity. Therefore, protocols to
381 isolate mitochondria need to be optimized according to each study. The term mitochondrial
382 preparation does not include further fractionation of mitochondrial components, neither
383 submitochondrial particles.

384

385 *2.1. Respiratory control and coupling*

386

387 Respiratory coupling control states are established in studies of mitochondrial
388 preparations to obtain reference values for various output variables. Physiological conditions *in*
389 *vivo* deviate from these experimentally obtained states. Since kinetically-saturating
390 concentrations, *e.g.*, of ADP or oxygen (O₂; dioxygen), may not apply to physiological
391 intracellular conditions, relevant information is obtained in studies of kinetic responses to
392 variations in [ADP] or [O₂] in the range between kinetically-saturating concentrations and
393 anoxia (Gnaiger 2001).

394 **The steady-state:** Mitochondria represent a thermodynamically open system in non-
395 equilibrium states of biochemical energy transformation. State variables (protonmotive force;
396 redox states) and metabolic *rates* (fluxes) are measured in defined mitochondrial respiratory
397 *states*. Steady-states can be obtained only in open systems, in which changes by *internal*
398 transformations, *e.g.*, O₂ consumption, are instantaneously compensated for by *external* fluxes,
399 *e.g.*, O₂ supply, preventing a change of O₂ concentration in the system (Gnaiger 1993b).
400 Mitochondrial respiratory states monitored in closed systems satisfy the criteria of pseudo-
401 steady states for limited periods of time, when changes in the system (concentrations of O₂, fuel
402 substrates, ADP, P_i, H⁺) do not exert significant effects on metabolic fluxes (respiration,
403 phosphorylation). Such pseudo-steady states require respiratory media with sufficient buffering
404 capacity and substrates maintained at kinetically-saturating concentrations, and thus depend on
405 the kinetics of the processes under investigation.

406 **Specification of biochemical dose:** Substrates, uncouplers, inhibitors, and other
407 chemical reagents are titrated to dissect mitochondrial function. Nominal concentrations of
408 these substances are usually reported as initial amount of substance concentration [mol·L⁻¹] in
409 the incubation medium. When aiming at the measurement of kinetically saturated processes—

410 such as OXPHOS-capacities, the concentrations for substrates can be chosen according to the
 411 apparent equilibrium constant, K_m' . In the case of hyperbolic kinetics, only 80% of maximum
 412 respiratory capacity is obtained at a substrate concentration of four times the K_m' , whereas
 413 substrate concentrations of 5, 9, 19 and 49 times the K_m' are theoretically required for reaching
 414 83%, 90%, 95% or 98% of the maximal rate (Gnaiger 2001). Other reagents are chosen to
 415 inhibit or alter some processes. The amount of these chemicals in an experimental incubation
 416 is selected to maximize effect, avoiding unacceptable off-target consequences that would
 417 adversely affect the data being sought. Specifying the amount of substance in an incubation as
 418 nominal concentration in the aqueous incubation medium can be ambiguous (Doskey *et al.*
 419 2015), particularly for lipophilic substances (oligomycin, uncouplers, permeabilization agents)
 420 or cations (TPP⁺; fluorescent dyes such as safranin, TMRM), which accumulate in biological
 421 membranes or in the mitochondrial matrix. For example, a dose of digitonin of 8 fmol·cell⁻¹ (10
 422 pg·cell⁻¹; 10 μg·10⁻⁶ cells) is optimal for permeabilization of endothelial cells, and the
 423 concentration in the incubation medium has to be adjusted according to the cell density applied
 424 (Doerrier *et al.* 2018).

425 Generally, dose/exposure can be specified per unit of biological sample, *i.e.*, (nominal
 426 moles of xenobiotic)/(number of cells) [mol·cell⁻¹] or, as appropriate, per mass of biological
 427 sample [mol·kg⁻¹]. This approach to specification of dose/exposure provides a scalable
 428 parameter that can be used to design experiments, help interpret a wide variety of experimental
 429 results, and provide absolute information that allows researchers worldwide to make the most
 430 use of published data (Doskey *et al.* 2015).

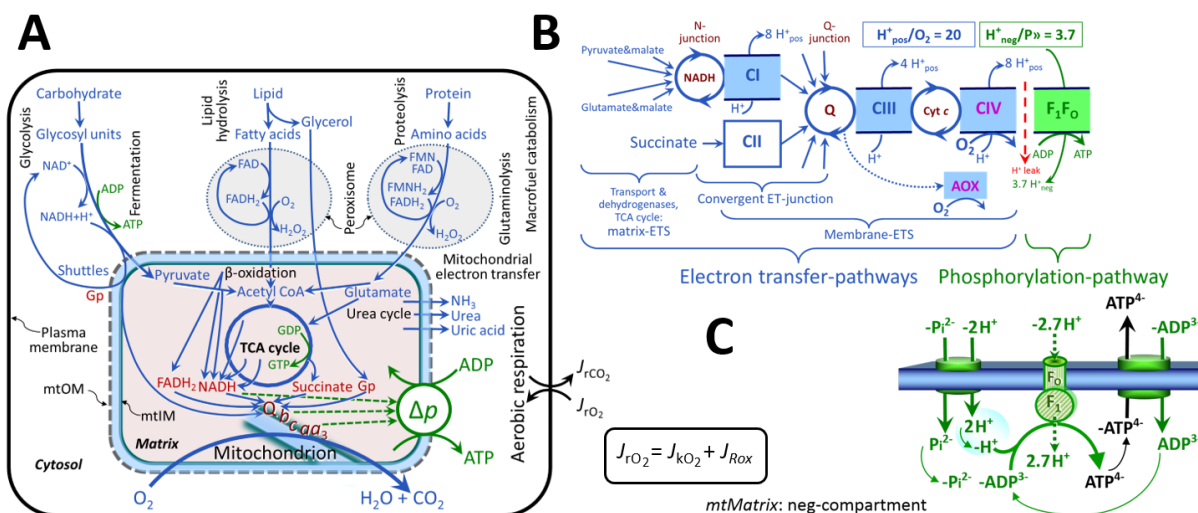
431 **Phosphorylation, P \gg , and P \gg /O $_2$ ratio:** *Phosphorylation* in the context of OXPHOS is
 432 defined as phosphorylation of ADP by P_i to form ATP. On the other hand, the term
 433 phosphorylation is used generally in many contexts, *e.g.*, protein phosphorylation. This justifies
 434 consideration of a symbol more discriminating and specific than P as used in the P/O ratio
 435 (phosphate to atomic oxygen ratio), where P indicates phosphorylation of ADP to ATP or GDP
 436 to GTP (**Figure 2**). We propose the symbol P \gg for the endergonic (uphill) direction of
 437 phosphorylation ADP→ATP, and likewise the symbol P \ll for the corresponding exergonic
 438 (downhill) hydrolysis ATP→ADP (**Figure 3**). P \gg refers mainly to electrontransfer
 439 phosphorylation but may also involve substrate-level phosphorylation as part of the
 440 tricarboxylic acid (TCA) cycle (succinyl-CoA ligase; phosphoglycerate kinase) and
 441 phosphorylation of ADP catalyzed by pyruvate kinase, and of GDP phosphorylated by
 442 phosphoenolpyruvate carboxykinase. Transphosphorylation is performed by adenylate kinase,
 443 creatine kinase, hexokinase and nucleoside diphosphate kinase. In isolated mammalian
 444 mitochondria, ATP production catalyzed by adenylate kinase (2 ADP ↔ ATP + AMP) proceeds
 445 without fuel substrates in the presence of ADP (Komlódi and Tretter 2017). Kinase cycles are
 446 involved in intracellular energy transfer and signal transduction for regulation of energy flux.

447 The P \gg /O $_2$ ratio (P \gg /4 e⁻) is two times the 'P/O' ratio (P \gg /2 e⁻) of classical bioenergetics.
 448 P \gg /O $_2$ is a generalized symbol, not specific for determination of P_i consumption (P_i/O $_2$ flux
 449 ratio), ADP depletion (ADP/O $_2$ flux ratio), or ATP production (ATP/O $_2$ flux ratio). The
 450 mechanistic P \gg /O $_2$ ratio—or P \gg /O $_2$ stoichiometry—is calculated from the proton-to-O $_2$ and
 451 proton-to-phosphorylation coupling stoichiometries (**Figure 2B**):
 452

$$453 \quad P\gg/O_2 = \frac{H_{pos}^+/O_2}{H_{neg}^+/P\gg} \quad (1)$$

454
 455 The H⁺_{pos}/O $_2$ *coupling stoichiometry* (referring to the full 4 electron reduction of O $_2$) depends
 456 on the ET-pathway control state, which defines the relative involvement of the three coupling
 457 sites (CI, CIII and CIV) in the catabolic pathway of electrons from the oxidation of reduced
 458 fuel substrates to the reduction of O $_2$. This varies with: (1) a bypass of CI by single or multiple
 459 electron input into the Q-junction; and (2) a bypass of CIV by involvement of alternative
 460 oxidases, AOX, which are not expressed in mammalian mitochondria.

461



462

463

Figure 2. Cell respiration and oxidative phosphorylation (OXPHOS)

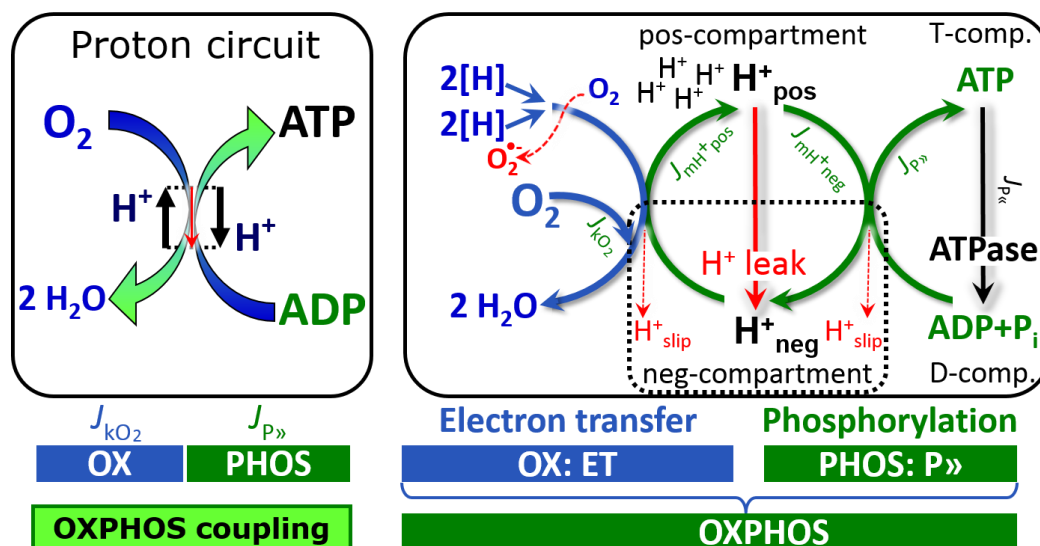
464 Mitochondrial respiration is the oxidation of fuel substrates with electron transfer to O_2 as the
 465 electron acceptor. For explanation of symbols see also **Figure 1**.

466 **(A)** Respiration in intact cells: Extra-mitochondrial catabolism of macrofuels or uptake of small
 467 molecules by the cell provides the *mitochondrial* fuel substrates. Many fuel substrates are
 468 catabolized to acetyl-CoA or glutamate, and further electron transfer reduces nicotinamide
 469 adenine dinucleotide to NADH or flavin adenine dinucleotide to $FADH_2$. In aerobic respiration,
 470 electron transfer is coupled to the phosphorylation of ADP to ATP, with energy transformation
 471 mediated by the protonmotive force, Δp . Anabolic reactions are linked to catabolism, both by
 472 ATP as the intermediary energy currency and by small organic precursor molecules as building
 473 blocks for biosynthesis (not shown). Glycolysis involves substrate-level phosphorylation of
 474 ADP to ATP in fermentation without utilization of O_2 . In contrast, extra-mitochondrial
 475 oxidation of fatty acids and amino acids proceeds partially in peroxisomes without coupling to
 476 ATP production: acyl-CoA oxidase catalyzes the oxidation of $FADH_2$ with electron transfer to
 477 O_2 ; amino acid oxidases oxidize flavin mononucleotide $FMNH_2$ or $FADH_2$. Coenzyme Q, Q,
 478 and the cytochromes *b*, *c*, and *aa₃* are redox systems of the mitochondrial inner membrane,
 479 mtIM. Dashed arrows indicate the connection between the redox proton pumps (respiratory
 480 Complexes CI, CIII and CIV) and the transmembrane Δp . Mitochondrial outer membrane,
 481 mtOM; glycerol-3-phosphate, Gp; tricarboxylic acid cycle, TCA cycle.

482 **(B)** Respiration in mitochondrial preparations: The mitochondrial electron transfer system
 483 (ETS) is fuelled by diffusion and transport of substrates across the mitochondrial outer and
 484 inner membrane and consists of the matrix-ETS and membrane-ETS. ET-pathways are coupled
 485 to the phosphorylation-pathway. ET-pathways converge at the N-junction and Q-junction.
 486 Additional arrows indicate electron entry into the Q-junction through electron transferring
 487 flavoprotein, glycerophosphate dehydrogenase, dihydro-orotate dehydrogenase, choline
 488 dehydrogenase, and sulfide-ubiquinone oxidoreductase. The dotted arrow indicates the
 489 branched pathway of oxygen consumption by alternative quinol oxidase (AOX). The H^+_{pos}/O_2
 490 ratio is the outward proton flux from the matrix space to the positively (pos) charged vesicular
 491 compartment, divided by catabolic O_2 flux in the NADH-pathway. The H^+_{neg}/P ratio is the
 492 inward proton flux from the inter-membrane space to the negatively (neg) charged matrix space,
 493 divided by the flux of phosphorylation of ADP to ATP. These are not fixed stoichiometries due
 494 to ion leaks and proton slip.

495 **(C)** Phosphorylation-pathway catalyzed by the proton pump F_1F_0 -ATPase (F-ATPase, ATP
 496 synthase), adenine nucleotide translocase, and inorganic phosphate transporter. The H^+_{neg}/P
 497 stoichiometry is the sum of the coupling stoichiometry in the F-ATPase reaction ($-2.7 H^+_{pos}$
 498 from the positive intermembrane space, $2.7 H^+_{neg}$ to the matrix, *i.e.*, the negative compartment)

499 and the proton balance in the translocation of ADP^{3-} , ATP^{4-} and P_i^{2-} . Modified from (B)
 500 Lemieux *et al.* (2017) and (C) Gnaiger (2014).
 501



502 **Figure 3. Coupling in oxidative phosphorylation (OXPHOS)**
 503 $2[\text{H}]$ indicates the reduced hydrogen equivalents of fuel substrates of the catabolic reaction k
 504 with oxygen. O_2 flux, $J_{k\text{O}_2}$, through the catabolic ET-pathway, is coupled to flux through the
 505 phosphorylation-pathway of ADP to ATP, $J_{P\gg}$. The redox proton pumps of the ET-pathway
 506 drive proton flux into the positive (pos) compartment, $J_{m\text{H}^+\text{pos}}$, generating the output
 507 protonmotive force (motive, subscript m). F-ATPase is coupled to inward proton current into
 508 the negative (neg) compartment, $J_{m\text{H}^+\text{neg}}$, to phosphorylate $\text{ADP}+\text{P}_i$ to ATP. The system is
 509 defined by the boundaries (full black line) and is not a black box, but is analysed as a
 510 compartmental system. The negative compartment (neg-compartment, enclosed by the dotted
 511 line) is the matrix space, separated by the mtIM from the positive compartment (pos-
 512 compartment). $\text{ADP}+\text{P}_i$ and ATP are the substrate- and product-compartments (scalar ADP and
 513 ATP compartments, D-comp. and T-comp.), respectively. At steady-state proton turnover,
 514 $J_{\infty\text{H}^+}$, and ATP turnover, $J_{\infty\text{P}}$, maintain concentrations constant, when $J_{m\text{H}^+\infty} = J_{m\text{H}^+\text{pos}} = J_{m\text{H}^+\text{neg}}$,
 515 and $J_{P\gg} = J_{P\ll} = J_{P\ll}$. Modified from Gnaiger (2014).
 516

517 $\text{H}^+_{\text{pos}}/\text{O}_2$ is 12 in the ET-pathways involving CIII and CIV as proton pumps, increasing to
 518 20 for the NADH-pathway (**Figure 2B**), but a general consensus on $\text{H}^+_{\text{pos}}/\text{O}_2$ stoichiometries
 519 remains to be reached (Hinkle 2005; Wikström and Hummer 2012; Sazanov 2015). The
 520 $\text{H}^+_{\text{neg}}/\text{P}\gg$ coupling stoichiometry (3.7; **Figure 2B**) is the sum of 2.7 H^+_{neg} required by the F-
 521 ATPase of vertebrate and most invertebrate species (Watt *et al.* 2010) and the proton balance
 522 in the translocation of ADP, ATP and P_i (**Figure 2C**). Taken together, the mechanistic $\text{P}\gg/\text{O}_2$
 523 ratio is calculated at 5.4 and 3.3 for NADH- and succinate-linked respiration, respectively (Eq.
 524 1). The corresponding classical $\text{P}\gg/\text{O}$ ratios (referring to the 2 electron reduction of 0.5O_2) are
 525 2.7 and 1.6 (Watt *et al.* 2010), in agreement with the measured $\text{P}\gg/\text{O}$ ratio for succinate of 1.58
 526 ± 0.02 (Gnaiger *et al.* 2000).

527 The effective $\text{P}\gg/\text{O}_2$ flux ratio ($Y_{\text{P}\gg/\text{O}_2} = J_{\text{P}\gg}/J_{k\text{O}_2}$; **Figure 3**) is diminished relative to the
 528 mechanistic $\text{P}\gg/\text{O}_2$ ratio by intrinsic and extrinsic uncoupling and dyscoupling (**Figure 4**). Such
 529 generalized uncoupling is different from switching to mitochondrial pathways that involve
 530 fewer than three proton pumps ('coupling sites': Complexes CI, CIII and CIV), bypassing CI
 531 through multiple electron entries into the Q-junction, or CIII and CIV through AOX (**Figure**
 532 **2B**). Reprogramming of mitochondrial pathways leading to different types of substrates being
 533 oxidized may be considered as a switch of gears (changing the stoichiometry by altering the
 534 substrate that is oxidized) rather than uncoupling (loosening the tightness of coupling relative

535 to a fixed stoichiometry). In addition, $Y_{P\gg O_2}$ depends on several experimental conditions of flux
 536 control, increasing as a hyperbolic function of [ADP] to a maximum value (Gnaiger 2001).

537 **Control and regulation:** The terms metabolic *control* and *regulation* are frequently used
 538 synonymously, but are distinguished in metabolic control analysis: ‘We could understand the
 539 regulation as the mechanism that occurs when a system maintains some variable constant over
 540 time, in spite of fluctuations in external conditions (homeostasis of the internal state). On the
 541 other hand, metabolic control is the power to change the state of the metabolism in response to
 542 an external signal’ (Fell 1997). Respiratory control may be induced by experimental control
 543 signals that *exert* an influence on: (1) ATP demand and ADP phosphorylation-rate; (2) fuel
 544 substrate composition, pathway competition; (3) available amounts of substrates and O₂, *e.g.*,
 545 starvation and hypoxia; (4) the protonmotive force, redox states, flux–force relationships,
 546 coupling and efficiency; (5) Ca²⁺ and other ions including H⁺; (6) inhibitors, *e.g.*, nitric oxide
 547 or intermediary metabolites such as oxaloacetate; (7) signalling pathways and regulatory
 548 proteins, *e.g.*, insulin resistance, transcription factor hypoxia inducible factor 1. *Mechanisms* of
 549 respiratory control and regulation include adjustments of: (1) enzyme activities by allosteric
 550 mechanisms and phosphorylation; (2) enzyme content, concentrations of cofactors and
 551 conserved moieties—such as adenylates, nicotinamide adenine dinucleotide [NAD⁺/NADH],
 552 coenzyme Q, cytochrome *c*; (3) metabolic channeling by supercomplexes; and (4)
 553 mitochondrial density (enzyme concentrations and membrane area) and morphology (cristae
 554 folding, fission and fusion). Mitochondria are targeted directly by hormones, thereby affecting
 555 their energy metabolism (Lee *et al.* 2013; Gerö and Szabo 2016; Price and Dai 2016; Moreno
 556 *et al.* 2017). Evolutionary or acquired differences in the genetic and epigenetic basis of
 557 mitochondrial function (or dysfunction) between subjects and gene therapy; age; gender,
 558 biological sex, and hormone concentrations; life style including exercise and nutrition; and
 559 environmental issues including thermal, atmospheric, toxicological and pharmacological
 560 factors, exert an influence on all control mechanisms listed above. For reviews, see Brown
 561 1992; Gnaiger 1993a, 2009; 2014; Paradies *et al.* 2014; Morrow *et al.* 2017.

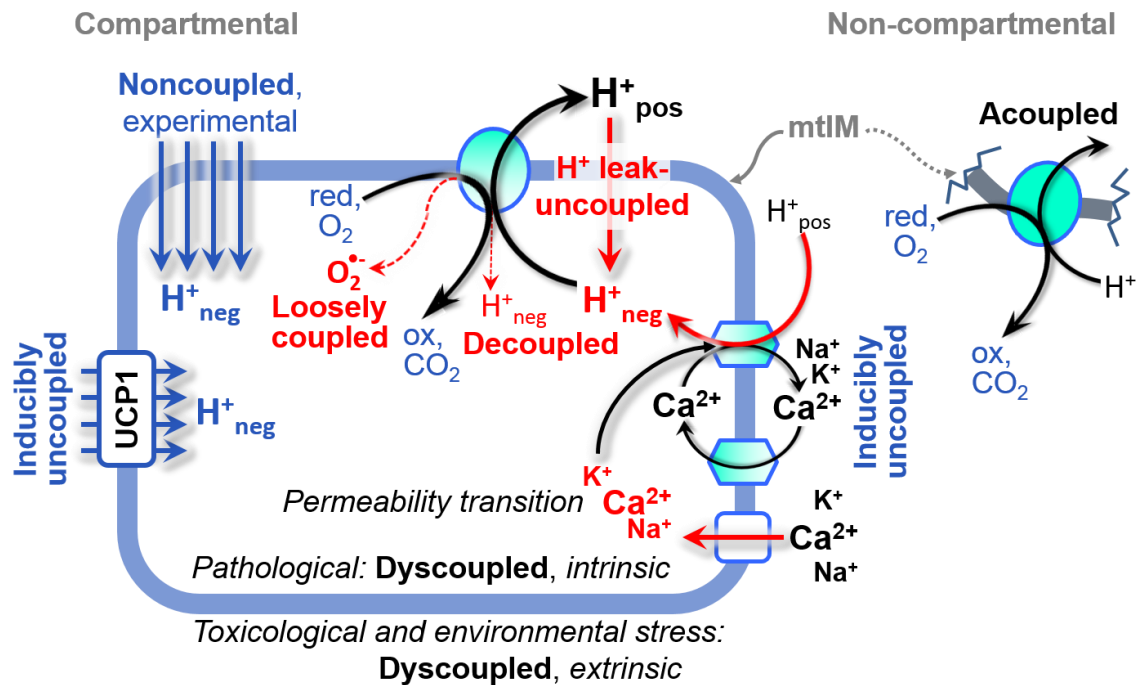
562 **Respiratory control and response:** Lack of control by a metabolic pathway, *e.g.*,
 563 phosphorylation-pathway, means that there will be no response to a variable activating it, *e.g.*,
 564 [ADP]. The reverse, however, is not true as the absence of a response to [ADP] does not exclude
 565 the phosphorylation-pathway from having some degree of control. The degree of control of a
 566 component of the OXPHOS-pathway on an output variable—such as O₂ flux, will in general
 567 be different from the degree of control on other outputs—such as phosphorylation-flux or
 568 proton leak flux. Therefore, it is necessary to be specific as to which input and output are under
 569 consideration (Fell 1997).

570 **Respiratory coupling control and ET-pathway control:** Respiratory control refers to
 571 the ability of mitochondria to adjust O₂ flux in response to external control signals by engaging
 572 various mechanisms of control and regulation. Respiratory control is monitored in a
 573 mitochondrial preparation under conditions defined as respiratory states. When
 574 phosphorylation of ADP to ATP is stimulated or depressed, an increase or decrease is observed
 575 in electron transfer measured as O₂ flux in respiratory coupling states of intact mitochondria
 576 (‘controlled states’ in the classical terminology of bioenergetics). Alternatively, coupling of
 577 electron transfer with phosphorylation is disengaged by uncouplers. These protonophores are
 578 weak lipid-soluble acids which disrupt the barrier function of the mtIM and thus shortcircuit
 579 the protonmotive system, functioning like a clutch in a mechanical system. The corresponding
 580 coupling control state is characterized by a high O₂ flux without control by P_» (‘uncontrolled
 581 state’).

582 ET-pathway control states are obtained in mitochondrial preparations by depletion of
 583 endogenous substrates and addition to the mitochondrial respiration medium of fuel substrates
 584 (2[H] in **Figure 3**) and specific inhibitors, activating selected mitochondrial catabolic pathways,
 585 *k*, of electron transfer from the oxidation of fuel substrates to reduction of O₂ (**Figure 2A**).

586 Coupling control states and pathway control states are complementary, since mitochondrial
 587 preparations depend on an exogenous supply of pathway-specific fuel substrates and oxygen
 588 (Gnaiger 2014).

589 **Coupling:** In mitochondrial electron transfer, vectorial transmembrane proton flux is
 590 coupled through the redox proton pumps CI, CIII and CIV to the catabolic flux of scalar
 591 reactions, collectively measured as O_2 flux (**Figure 3**). Thus mitochondria are elements of
 592 energy transformation. Energy is a conserved quantity and cannot be lost or produced in any
 593 internal process (First Law of thermodynamics). Open and closed systems can gain or lose
 594 energy only by external fluxes—by exchange with the environment. Therefore, energy can
 595 neither be produced by mitochondria, nor is there any internal process without energy
 596 conservation. Exergy is defined as the Gibbs energy ('free energy') with the potential to
 597 perform work under conditions of constant volume and pressure. *Coupling* is the interaction of
 598 an exergonic process (spontaneous, negative exergy change) with an endergonic process
 599 (positive exergy change) in energy transformations which conserve part of the exergy that
 600 would be irreversibly lost or dissipated in an uncoupled process.
 601



602

603

604 **Figure 4. Mechanisms of respiratory uncoupling**

605

606

607

608

609

610

611

612

613

614

615

616 **Uncoupling:** Uncoupling of mitochondrial respiration is a general term comprising
 617 diverse mechanisms:

618

1. Proton leak across the mtIM from the pos- to the neg-compartment (**Figure 3**);
2. Cycling of other cations, strongly stimulated by permeability transition, or experimentally induced by valinomycin in the presence of K^+ ;

618

- 619 3. Proton slip in the redox proton pumps when protons are effectively not pumped (CI,
620 CIII and CIV) or are not driving phosphorylation (F-ATPase);
621 4. Loss of vesicular (compartmental) integrity when electron transfer is acoupled;
622 5. Electron leak in the loosely coupled univalent reduction of O_2 to superoxide ($O_2^{\cdot-}$;
623 superoxide anion radical).

624 Differences of terms—uncoupled vs. noncoupled—are easily overlooked, although they relate
625 to different meanings of uncoupling (**Figure 4**).

626

627 2.2. Coupling states and respiratory rates

628

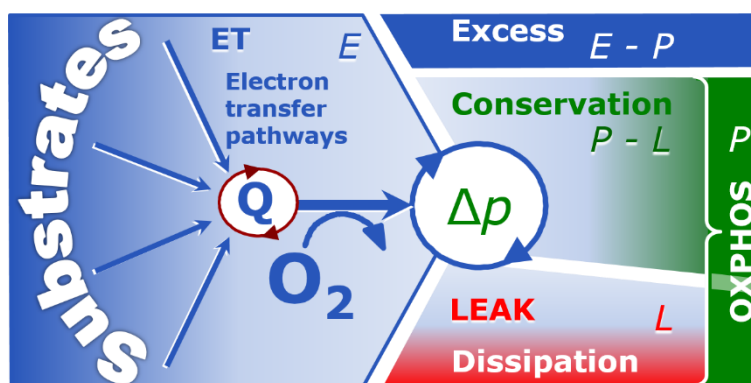
629 **Respiratory capacities in coupling control states:** To extend the classical nomenclature
630 on mitochondrial coupling states (Section 2.3) by a concept-driven terminology that explicitly
631 incorporates information on the meaning of respiratory states, the terminology must be general
632 and not restricted to any particular experimental protocol or mitochondrial preparation (Gnaiger
633 2009). Concept-driven nomenclature aims at mapping the *meaning and concept behind* the
634 words and acronyms onto the *forms* of words and acronyms (Miller 1991). The focus of
635 concept-driven nomenclature is primarily the conceptual ‘why’, along with clarification of the
636 experimental ‘how’. Respiratory capacities delineate, comparable to channel capacity in
637 information theory (Schneider 2006), the upper bound of the rate of respiration measured in
638 defined coupling control states and electron transfer-pathway (ET-pathway) states (**Figure 5**).

639 To provide a diagnostic reference for respiratory capacities of core energy metabolism,
640 the capacity of *oxidative phosphorylation*, OXPHOS, is measured at kinetically-saturating
641 concentrations of ADP and P_i . The *oxidative* ET-capacity reveals the limitation of OXPHOS-
642 capacity mediated by the *phosphorylation*-pathway. The ET- and phosphorylation-pathways
643 comprise coupled segments of the OXPHOS-system. ET-capacity is measured as noncoupled
644 respiration by application of *external uncouplers*. The contribution of *intrinsically uncoupled*
645 O_2 consumption is studied by preventing the stimulation of phosphorylation either in the
646 absence of ADP or by inhibition of the phosphorylation-pathway. The corresponding states are
647 collectively classified as LEAK-states, when O_2 consumption compensates mainly for ion
648 leaks, including the proton leak. Defined coupling states are induced by: (1) adding cation
649 chelators such as EGTA, binding free Ca^{2+} and thus limiting cation cycling; (2) adding ADP
650 and P_i ; (3) inhibiting the phosphorylation-pathway; and (4) uncoupler titrations, while
651 maintaining a defined ET-pathway state with constant fuel substrates and inhibitors of specific
652 branches of the ET-pathway (**Figure 5**).

653

654 **Figure 5. Four-compartment model of oxidative phosphorylation**

655 Respiratory states (ET, OXPHOS, LEAK; **Table 1**) and corresponding rates (E , P , L) are
656 connected by the protonmotive force, Δp . ET-capacity, E (1), is partitioned into (2) dissipative
657 LEAK-respiration, L , when the Gibbs energy change of catabolic
658 O_2 flux is irreversibly lost, (3) net OXPHOS-capacity, $P-L$, with partial conservation of the
659 capacity to perform work, and (4) the excess capacity, $E-P$. Modified from Gnaiger (2014).
660
661
662
663
664
665
666
667



668 The three coupling states, ET, LEAK and OXPHOS, are shown schematically with the
669 corresponding respiratory rates, abbreviated as E , L and P , respectively (**Figure 5**). We

670 distinguish metabolic *pathways* from metabolic *states* and the corresponding metabolic *rates*;
 671 for example: ET-pathways (**Figure 5**), ET-states (**Figure 6C**), and ET-capacities, E ,
 672 respectively (**Table 1**). The protonmotive force is *high* in the OXPHOS-state when it drives
 673 phosphorylation, *maximum* in the LEAK-state of coupled mitochondria, driven by LEAK-
 674 respiration at a minimum back flux of cations to the matrix side, and *very low* in the ET-state
 675 when uncouplers short-circuit the proton cycle (**Table 1**).

676
 677
 678
 679
 680

Table 1. Coupling states and residual oxygen consumption in mitochondrial preparations in relation to respiration- and phosphorylation-flux, J_{KO_2} and J_{P} , and protonmotive force, Δp . Coupling states are established at kinetically-saturating concentrations of fuel substrates and O_2 .

State	J_{KO_2}	J_{P}	Δp	Inducing factors	Limiting factors
LEAK	L ; low, cation leak-dependent respiration	0	max.	proton leak, slip, and cation cycling	$J_{\text{P}} = 0$: (1) without ADP, L_N ; (2) max. ATP/ADP ratio, L_T ; or (3) inhibition of the phosphorylation-pathway, L_{omy}
OXPHOS	P ; high, ADP-stimulated respiration	max.	high	kinetically-saturating [ADP] and [P_i]	J_{P} by phosphorylation-pathway; or J_{KO_2} by ET-capacity
ET	E ; max., noncoupled respiration	0	low	optimal external uncoupler concentration for max. $J_{\text{O}_2, E}$	J_{KO_2} by ET-capacity
ROX	R_{ox} ; min., residual O_2 consumption	0	0	$J_{\text{O}_2, R_{\text{ox}}}$ in non-ET-pathway oxidation reactions	inhibition of all ET-pathways; or absence of fuel substrates

681

682 **LEAK-state (Figure 6A):** The LEAK-state is defined as a state of mitochondrial
 683 respiration when O_2 flux mainly compensates for ion leaks in the absence of ATP synthesis, at
 684 kinetically-saturating concentrations of O_2 and respiratory fuel substrates. LEAK-respiration is
 685 measured to obtain an estimate of *intrinsic uncoupling* without addition of an experimental
 686 uncoupler: (1) in the absence of adenylates, *i.e.*, AMP, ADP and ATP; (2) after depletion of
 687 ADP at a maximum ATP/ADP ratio; or (3) after inhibition of the phosphorylation-pathway by
 688 inhibitors of F-ATPase—such as oligomycin, or of adenine nucleotide translocase—such as
 689 carboxyatractyloside. Adjustment of the nominal concentration of these inhibitors to the density
 690 of biological sample applied can minimize or avoid inhibitory side-effects exerted on ET-
 691 capacity or even some dyscoupling.

692 **Proton leak and uncoupled respiration:** Proton leak is a leak current of protons. The
 693 intrinsic proton leak is the *uncoupled* process in which protons diffuse across the mtIM in the
 694 dissipative direction of the downhill protonmotive force without coupling to phosphorylation
 695 (**Figure 6A**). The proton leak flux depends non-linearly on the protonmotive force (Garlid *et*
 696 *al.* 1989; Divakaruni and Brand 2011), it is a property of the mtIM and may be enhanced due
 697 to possible contaminations by free fatty acids. Inducible uncoupling mediated by uncoupling
 698 protein 1 (UCP1) is physiologically controlled, *e.g.*, in brown adipose tissue. UCP1 is a member
 699 of the mitochondrial carrier family which is involved in the translocation of protons across the

700 mtIM (Klingenberg 2017). Consequently, the short-circuit diminishes the protonmotive force
701 and stimulates electron transfer to O₂ and heat dissipation without phosphorylation of ADP.

702 **Cation cycling:** There can be other cation contributors to leak current including calcium
703 and probably magnesium. Calcium current is balanced by mitochondrial Na⁺/Ca²⁺ exchange,
704 which is balanced by Na⁺/H⁺ or K⁺/H⁺ exchanges. This is another effective uncoupling
705 mechanism different from proton leak (**Table 2**).

706
707

Table 2. Terms on respiratory coupling and uncoupling.

Term	J_{kO_2}	$P \gg O_2$	Note	
acoupled		0	electron transfer in mitochondrial fragments without vectorial proton translocation (Figure 4)	
intrinsic, no protonophore added	uncoupled	L	0	non-phosphorylating LEAK-respiration (Figure 6A)
	proton leak-uncoupled		0	component of L , H ⁺ diffusion across the mtIM (Figure 4)
	decoupled		0	component of L , proton slip (Figure 4)
	loosely coupled		0	component of L , lower coupling due to superoxide formation and bypass of proton pumps (Figure 4)
	dyscoupled		0	pathologically, toxicologically, environmentally increased uncoupling, mitochondrial dysfunction
	inducibly uncoupled		0	by UCP1 or cation (<i>e.g.</i> , Ca ²⁺) cycling (Figure 4)
noncoupled	E	0	non-phosphorylating respiration stimulated to maximum flux at optimum exogenous uncoupler concentration (Figure 6C)	
well-coupled	P	high	phosphorylating respiration with an intrinsic LEAK component (Figure 6B)	
fully coupled	$P - L$	max.	OXPPOS-capacity corrected for LEAK-respiration (Figure 5)	

708

709 **Proton slip and decoupled respiration:** Proton slip is the *decoupled* process in which
710 protons are only partially translocated by a redox proton pump of the ET-pathways and slip
711 back to the original vesicular compartment. The proton leak is the dominant contributor to the
712 overall leak current in mammalian mitochondria incubated under physiological conditions at
713 37 °C, whereas proton slip is increased at lower experimental temperature (Canton *et al.* 1995).
714 Proton slip can also happen in association with the F-ATPase, in which the proton slips downhill
715 across the pump to the matrix without contributing to ATP synthesis. In each case, proton slip
716 is a property of the proton pump and increases with the pump turnover rate.

717 **Electron leak and loosely coupled respiration:** Superoxide production by the ETS leads
718 to a bypass of redox proton pumps and correspondingly lower $P \gg O_2$ ratio. This depends on the
719 actual site of electron leak and the scavenging of hydrogen peroxide by cytochrome *c*, whereby
720 electrons may re-enter the ETS with proton translocation by CIV.

721 **Loss of compartmental integrity and acoupled respiration:** Electron transfer and
722 catabolic O₂ flux proceed without compartmental proton translocation in disrupted
723 mitochondrial fragments. Such fragments form during mitochondrial isolation, and may not
724 fully fuse to re-establish structurally intact mitochondria. Loss of mtIM integrity, therefore, is

725 the cause of acoupled respiration, which is a nonvectorial dissipative process without control
726 by the protonmotive force.

727 **Dyscoupled respiration:** Mitochondrial injuries may lead to *dyscoupling* as a
728 pathological or toxicological cause of *uncoupled* respiration. Dyscoupling may involve any
729 type of uncoupling mechanism, *e.g.*, opening the permeability transition pore. Dyscoupled
730 respiration is distinguished from the experimentally induced *noncoupled* respiration in the ET-
731 state (**Table 2**).

732
733 **OXPPOS-state (Figure 6B):** The OXPPOS-state is defined as the respiratory state
734 with kinetically-saturating concentrations of O_2 , respiratory and phosphorylation substrates,
735 and absence of exogenous uncoupler, which provides an estimate of the maximal
736 respiratory capacity in the OXPPOS-state for any given ET-pathway state. Respiratory
737 capacities at kinetically-saturating substrate concentrations provide reference
738 values or upper limits of performance, aiming at the generation of data sets for
739 comparative purposes. Physiological activities and effects of substrate kinetics can
740 be evaluated relative to the OXPPOS-capacity.

741 As discussed previously, 0.2 mM ADP does not fully saturate flux in isolated
742 mitochondria (Gnaiger 2001; Puchowicz *et al.* 2004); greater ADP concentration is required,
743 particularly in permeabilized muscle fibres and cardiomyocytes, to overcome
744 limitations by intracellular diffusion and by the reduced conductance of the mtOM
745 (Jepihhina *et al.* 2011, Illaste *et al.* 2012, Simson *et al.* 2016), either through interaction with
746 tubulin (Rostovtseva *et al.* 2008) or other intracellular structures (Birkedal *et al.* 2014). In
747 permeabilized muscle fibre bundles of high respiratory

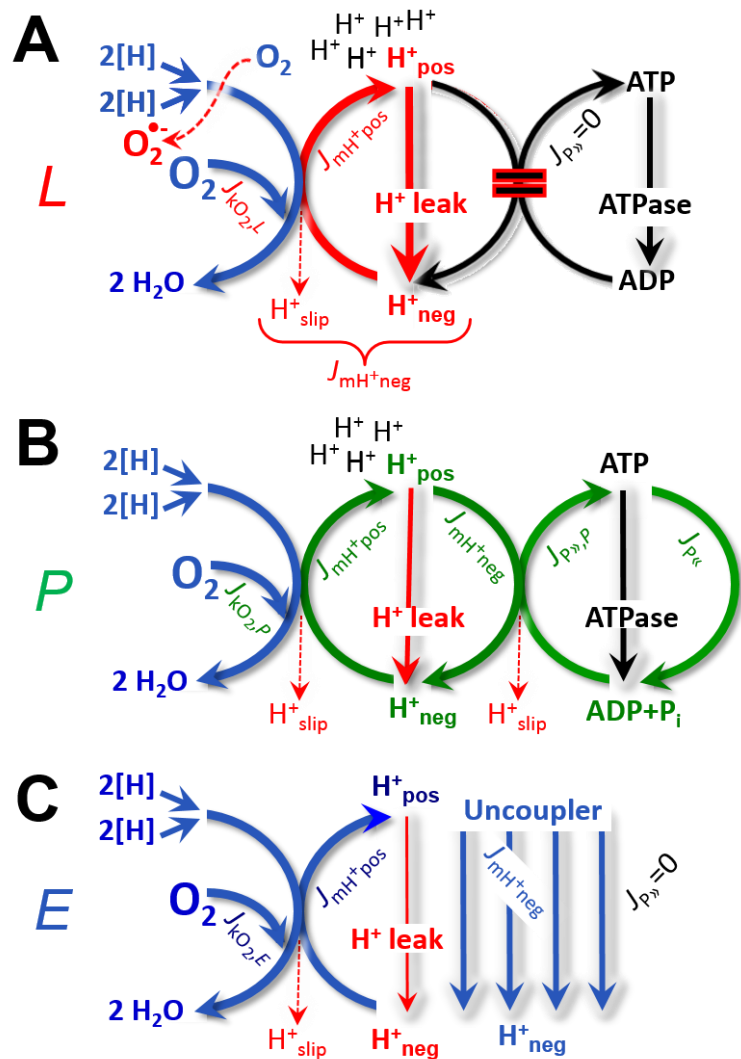


Figure 6. Respiratory coupling states

(A) **LEAK-state and rate, L:** Phosphorylation is arrested, $J_{P>} = 0$, and catabolic O_2 flux, $J_{kO_2,L}$, is controlled mainly by the proton leak, $J_{mH^+neg,L}$, at maximum protonmotive force (**Figure 4**).

(B) **OXPPOS-state and rate, P:** Phosphorylation, $J_{P>,P}$, is stimulated by kinetically-saturating $[ADP]$ and $[P_i]$, and is supported by a high protonmotive force. O_2 flux, $J_{kO_2,P}$, is well-coupled at a $P>/O_2$ ratio of $J_{P>,P}/J_{kO_2,P}$.

(C) **ET-state and rate, E:** Noncoupled respiration, $J_{kO_2,E}$, is maximum at optimum exogenous uncoupler concentration and phosphorylation is zero, $J_{P>} = 0$. See also **Figure 3**.

776 capacity, the apparent K_m for ADP increases up to 0.5 mM (Saks *et al.* 1998), consistent with
 777 experimental evidence that >90% saturation is reached only at >5 mM ADP (Pesta and Gnaiger
 778 2012). Similar ADP concentrations are also required for accurate determination of OXPHOS-
 779 capacity in human clinical cancer samples and permeabilized cells (Klepinin *et al.* 2016; Koit
 780 *et al.* 2017). Whereas 2.5 to 5 mM ADP is sufficient to obtain the actual OXPHOS-capacity in
 781 many types of permeabilized tissue and cell preparations, experimental validation is required
 782 in each specific case.

783 **Electron transfer-state (Figure 6C):** The ET-state is defined as the *noncoupled* state
 784 with kinetically-saturating concentrations of O₂, respiratory substrate and optimum *exogenous*
 785 uncoupler concentration for maximum O₂ flux. O₂ flux determined in the ET-state yields an
 786 estimate of ET-capacity. Inhibition of respiration is observed above optimum uncoupler
 787 concentrations. As a consequence of the nearly collapsed protonmotive force, the driving force
 788 is insufficient for phosphorylation, and $J_{P_{\infty}} = 0$.

789 **ROX state and Rox:** Besides the three fundamental coupling states of mitochondrial
 790 preparations, the state of residual O₂ consumption, ROX, is relevant to assess respiratory
 791 function (Figure 1). ROX is not a coupling state. The rate of residual oxygen consumption,
 792 *Rox*, is defined as O₂ consumption due to oxidative reactions measured after inhibition of ET—
 793 with rotenone, malonic acid and antimycin A. Cyanide and azide inhibit not only CIV but
 794 catalase and several peroxidases involved in *Rox*. However, high concentrations of antimycin
 795 A, but not rotenone or cyanide, inhibit peroxisomal acyl-CoA oxidase and D-amino acid
 796 oxidase (Vamecq *et al.* 1987). ROX represents a baseline that is used to correct respiration
 797 measured in defined coupling states. *Rox*-corrected *L*, *P* and *E* not only lower the values of total
 798 fluxes, but also changes the flux control ratios *L/P* and *L/E*. *Rox* is not necessarily equivalent
 799 to non-mitochondrial reduction of O₂, considering O₂-consuming reactions in mitochondria that
 800 are not related to ET—such as O₂ consumption in reactions catalyzed by monoamine oxidases
 801 (type A and B), monooxygenases (cytochrome P450 monooxygenases), dioxygenase (sulfur
 802 dioxygenase and trimethyllysine dioxygenase), and several hydroxylases. Even isolated
 803 mitochondrial fractions, especially those obtained from liver, may be contaminated by
 804 peroxisomes. This fact makes the exact determination of mitochondrial O₂ consumption and
 805 mitochondria-associated generation of reactive oxygen species complicated (Schönfeld *et al.*
 806 2009; Speijer 2016; Figure 2). The dependence of ROX-linked O₂ consumption needs to be
 807 studied in detail together with non-ET enzyme activities, availability of specific substrates, O₂
 808 concentration, and electron leakage leading to the formation of reactive oxygen species.

809 **Quantitative relations:** *E* may exceed or be equal to *P*. $E > P$ is observed in many types
 810 of mitochondria, varying between species, tissues and cell types (Gnaiger 2009). $E - P$ is the
 811 excess ET-capacity pushing the phosphorylation-flux (Figure 2C) to the limit of its *capacity of*
 812 *utilizing* the protonmotive force. In addition, the magnitude of $E - P$ depends on the tightness of
 813 respiratory coupling or degree of uncoupling, since an increase of *L* causes *P* to increase
 814 towards the limit of *E*. The *excess E-P* capacity, $E - P$, therefore, provides a sensitive diagnostic
 815 indicator of specific injuries of the phosphorylation-pathway, under conditions when *E* remains
 816 constant but *P* declines relative to controls (Figure 5). Substrate cocktails supporting
 817 simultaneous convergent electron transfer to the Q-junction for reconstitution of TCA cycle
 818 function establish pathway control states with high ET-capacity, and consequently increase the
 819 sensitivity of the $E - P$ assay.

820 *E* cannot theoretically be lower than *P*. $E < P$ must be discounted as an artefact, which
 821 may be caused experimentally by: (1) loss of oxidative capacity during the time course of the
 822 respirometric assay, since *E* is measured subsequently to *P*; (2) using insufficient uncoupler
 823 concentrations; (3) using high uncoupler concentrations which inhibit ET (Gnaiger 2008); (4)
 824 high oligomycin concentrations applied for measurement of *L* before titrations of uncoupler,
 825 when oligomycin exerts an inhibitory effect on *E*. On the other hand, the excess ET-capacity is
 826 overestimated if non-saturating [ADP] or [P_i] are used. See State 3 in the next section.

827 The net OXPHOS-capacity is calculated by subtracting L from P (**Figure 5**). The net
 828 P_{\gg}/O_2 equals $P_{\gg}/(P-L)$, wherein the dissipative LEAK component in the OXPHOS-state may
 829 be overestimated. This can be avoided by measuring LEAK-respiration in a state when the
 830 protonmotive force is adjusted to its slightly lower value in the OXPHOS-state—by titration of
 831 an ET inhibitor (Divakaruni and Brand 2011). Any turnover-dependent components of proton
 832 leak and slip, however, are underestimated under these conditions (Garlid *et al.* 1993). In
 833 general, it is inappropriate to use the term *ATP production* or *ATP turnover* for the difference
 834 of O_2 flux measured in the OXPHOS and LEAK states. $P-L$ is the upper limit of OXPHOS-
 835 capacity that is freely available for ATP production (corrected for LEAK-respiration) and is
 836 fully coupled to phosphorylation with a maximum mechanistic stoichiometry (**Figure 5**).

837 The rates of LEAK respiration and OXPHOS capacity depend on (1) the tightness of
 838 coupling under the influence of the respiratory uncoupling mechanisms (**Figure 4**), and (2) the
 839 coupling stoichiometry which varies as a function of the substrate type undergoing oxidation in
 840 ET-pathways with either two or three coupling sites (**Figure 2B**). When cocktails with NADH-
 841 linked substrates and succinate are used, the relative contribution of ET-pathways with three or
 842 two coupling sites cannot be controlled experimentally, is difficult to determine, and may shift
 843 in transitions between LEAK-, OXPHOS- and ET-states (Gnaiger 2014). Under these
 844 experimental conditions, we cannot separate the tightness of coupling *versus* coupling
 845 stoichiometry as the mechanisms of respiratory control in the shift of L/P ratios. The tightness
 846 of coupling and fully coupled O_2 flux, $P-L$ (**Table 2**), therefore, are obtained from
 847 measurements of coupling control of LEAK respiration, OXPHOS- and ET-capacities in well
 848 defined pathway states, using either pyruvate and malate as substrates or the classical succinate
 849 and rotenone substrate-inhibitor combination (**Figure 2B**).

850

851 2.3. Classical terminology for isolated mitochondria

852 ‘When a code is familiar enough, it ceases appearing like a code; one forgets that there
 853 is a decoding mechanism. The message is identical with its meaning’ (Hofstadter 1979).

854

855 Chance and Williams (1955; 1956) introduced five classical states of mitochondrial
 856 respiration and cytochrome redox states. **Table 3** shows a protocol with isolated mitochondria
 857 in a closed respirometric chamber, defining a sequence of respiratory states. States and rates
 858 are not specifically distinguished in this nomenclature.

859

860

861

862

Table 3. Metabolic states of mitochondria (Chance and Williams, 1956; Table V).

State	[O ₂]	ADP level	Substrate level	Respiration rate	Rate-limiting substance
1	>0	low	low	slow	ADP
2	>0	high	~0	slow	substrate
3	>0	high	high	fast	respiratory chain
4	>0	low	high	slow	ADP
5	0	high	high	0	oxygen

863

864 **State 1** is obtained after addition of isolated mitochondria to air-saturated
 865 isoosmotic/isotonic respiration medium containing P_i , but no fuel substrates and no adenylates,
 866 *i.e.*, AMP, ADP, ATP.

867 **State 2** is induced by addition of a ‘high’ concentration of ADP (typically 100 to 300
 868 μ M), which stimulates respiration transiently on the basis of endogenous fuel substrates and
 869 phosphorylates only a small portion of the added ADP. State 2 is then obtained at a low
 870 respiratory activity limited by exhausted endogenous fuel substrate availability (**Table 3**). If

871 addition of specific inhibitors of respiratory complexes—such as rotenone—does not cause a
 872 further decline of O₂ flux, State 2 is equivalent to the ROX state (See below.). If inhibition is
 873 observed, undefined endogenous fuel substrates are a confounding factor of pathway control,
 874 contributing to the effect of subsequently externally added substrates and inhibitors. In contrast
 875 to the original protocol, an alternative sequence of titration steps is frequently applied, in which
 876 the alternative ‘State 2’ has an entirely different meaning, when this second state is induced by
 877 addition of fuel substrate without ADP (LEAK-state; in contrast to State 2 defined in **Table 1**
 878 as a ROX state), followed by addition of ADP.

879 **State 3** is the state stimulated by addition of fuel substrates while the ADP concentration
 880 is still high (**Table 3**) and supports coupled energy transformation through oxidative
 881 phosphorylation. ‘High ADP’ is a concentration of ADP specifically selected to allow the
 882 measurement of State 3 to State 4 transitions of isolated mitochondria in a closed respirometric
 883 chamber. Repeated ADP titration re-establishes State 3 at ‘high ADP’. Starting at O₂
 884 concentrations near air-saturation (ca. 200 μM O₂ at sea level and 37 °C), the total ADP
 885 concentration added must be low enough (typically 100 to 300 μM) to allow phosphorylation
 886 to ATP at a coupled O₂ flux that does not lead to O₂ depletion during the transition to State 4.
 887 In contrast, kinetically-saturating ADP concentrations usually are 10-fold higher than ‘high
 888 ADP’, e.g., 2.5 mM in isolated mitochondria. The abbreviation State 3u is occasionally used in
 889 bioenergetics, to indicate the state of respiration after titration of an uncoupler, without
 890 sufficient emphasis on the fundamental difference between OXPHOS-capacity (*well-coupled*
 891 with an *endogenous* uncoupled component) and ET-capacity (*noncoupled*).

892 **State 4** is a LEAK-state that is obtained only if the mitochondrial preparation is intact
 893 and well-coupled. Depletion of ADP by phosphorylation to ATP causes a decline of O₂ flux in
 894 the transition from State 3 to State 4. Under the conditions of State 4, a maximum protonmotive
 895 force and high ATP/ADP ratio are maintained. The gradual decline of $Y_{P\gg/O_2}$ towards
 896 diminishing [ADP] at State 4 must be taken into account for calculation of $P\gg/O_2$ ratios (Gnaiger
 897 2001). State 4 respiration, L_T (**Table 1**), reflects intrinsic proton leak and ATP hydrolysis
 898 activity. O₂ flux in State 4 is an overestimation of LEAK-respiration if the contaminating ATP
 899 hydrolysis activity recycles some ATP to ADP, $J_{P\ll}$, which stimulates respiration coupled to
 900 phosphorylation, $J_{P\gg} > 0$. This can be tested by inhibition of the phosphorylation-pathway using
 901 oligomycin, ensuring that $J_{P\gg} = 0$ (State 4o). Alternatively, sequential ADP titrations re-
 902 establish State 3, followed by State 3 to State 4 transitions while sufficient O₂ is available.
 903 Anoxia may be reached, however, before exhaustion of ADP (State 5).

904 **State 5** is the state after exhaustion of O₂ in a closed respirometric chamber. Diffusion of
 905 O₂ from the surroundings into the aqueous solution may be a confounding factor preventing
 906 complete anoxia (Gnaiger 2001). Chance and Williams (1955) provide an alternative definition
 907 of State 5, which gives it the different meaning of ROX versus anoxia: ‘State 5 may be obtained
 908 by antimycin A treatment or by anaerobiosis’.

909 In **Table 3**, only States 3 and 4 (and ‘State 2’ in the alternative protocol: addition of fuel
 910 substrates without ADP; not included in the table) are coupling control states, with the
 911 restriction that O₂ flux in State 3 may be limited kinetically by non-saturating ADP
 912 concentrations (**Table 1**).

913

914

915 **3. Normalization: fluxes and flows**

916

917 *3.1. Normalization: system or sample*

918

919 The term *rate* is not sufficiently defined to be useful for reporting data (**Figure 7**). The
 920 inconsistency of the meanings of rate becomes fully apparent when considering Galileo
 921 Galilei’s famous principle, that ‘bodies of different weight all fall at the same rate (have a
 922 constant acceleration)’ (Coopersmith 2010).

923 **Flow per system, I :** In a generalization of electrical terms, flow as an extensive quantity
 924 (I ; per system) is distinguished from flux as a size-specific quantity (J ; per system size) (**Figure**
 925 **7A**). Electric current is flow, I_{el} [$A \equiv C \cdot s^{-1}$] per system (extensive quantity). When dividing this
 926 extensive quantity by system size (cross-sectional area of a ‘wire’), a size-specific quantity is
 927 obtained, which is flux (current density), J_{el} [$A \cdot m^{-2} = C \cdot s^{-1} \cdot m^{-2}$] (**Box 2**).
 928

929 **Box 2: Metabolic fluxes and flows: vectorial and scalar**

930
 931 Fluxes are *vectors*, if they have *spatial* geometric direction in addition to magnitude.
 932 Electric charge per unit time is electric flow or current, $I_{el} = dQ_{el} \cdot dt^{-1}$ [A]. When expressed per
 933 unit cross-sectional area, A [m^2], a vector flux is obtained, which is current density (surface-
 934 density of flow) perpendicular to the direction of flux, $J_{el} = I_{el} \cdot A^{-1}$ [$A \cdot m^{-2}$] (Cohen et al. 2008).
 935 For all transformations *flows*, I_{tr} , are defined as extensive quantities. Vector and scalar *fluxes*
 936 are obtained as $J_{tr} = I_{tr} \cdot A^{-1}$ [$mol \cdot s^{-1} \cdot m^{-2}$] and $J_{tr} = I_{tr} \cdot V^{-1}$ [$mol \cdot s^{-1} \cdot m^{-3}$], expressing flux as an area-
 937 specific vector or volume-specific vectorial or scalar quantity, respectively (Gnaiger 1993b).
 938 We use the metre–kilogram–second–ampere (MKSA) international system of units (*SI*) for
 939 general cases ([m], [kg], [s] and [A]), with decimal *SI* prefixes for specific applications (**Table**
 940 **4**).

941 We suggest to define: (1) *vectorial* fluxes, which are translocations as functions of
 942 *gradients* with direction in geometric space in continuous systems; (2) *vectorial* fluxes, which
 943 describe translocations in discontinuous systems and are restricted to information on
 944 *compartmental differences* (**Figure 3**, transmembrane proton flux); and (3) *scalar* fluxes, which
 945 are transformations in a *homogenous* system (**Figure 3**, catabolic O_2 flux, J_{kO_2}).

946 Vectorial transmembrane proton fluxes, J_{mH^+pos} and J_{mH^+neg} , are analyzed in a
 947 heterogenous compartmental system as a quantity with *directional* but not *spatial* information.
 948 Translocation of protons across the mtIM has a defined direction, either from the negative
 949 compartment (matrix space; negative, neg–compartment) to the positive compartment (inter-
 950 membrane space; positive, pos–compartment) or *vice versa* (**Figure 3**). The arrows defining
 951 the direction of the translocation between the two vesicular compartments may point upwards
 952 or downwards, right or left, without any implication that these are actual directions in space.
 953 The pos–compartment is neither above nor below the neg–compartment in a spatial sense, but
 954 can be visualized arbitrarily in a figure in the upper position (**Figure 3**). In general, the
 955 *compartmental direction* of vectorial translocation from the neg–compartment to the pos–
 956 compartment is defined by assigning the initial and final state as *ergodynamic compartments*,
 957 $H^+_{neg} \rightarrow H^+_{pos}$ or $0 = -1 H^+_{neg} + 1 H^+_{pos}$, related to work (erg = work) that must be performed to
 958 lift the proton from a lower to a higher electrochemical potential or from the lower to the higher
 959 ergodynamic compartment (Gnaiger 1993b).

960 In analogy to *vectorial* translocation, the direction of a *scalar* chemical reaction, $A \rightarrow B$
 961 or $0 = -1 A + 1 B$, is defined by assigning substrates and products, A and B, as ergodynamic
 962 compartments. O_2 is defined as a substrate in respiratory O_2 consumption, which together with
 963 the fuel substrates comprises the substrate compartment of the catabolic reaction. Volume-
 964 specific scalar O_2 flux is coupled to vectorial translocation, yielding the H^+_{pos}/O_2 ratio (**Figure**
 965 **2B**).

966
 967 **Extensive quantities:** An extensive quantity increases proportionally with system size.
 968 The magnitude of an extensive quantity is completely additive for non-interacting
 969 subsystems—such as mass or flow expressed per defined system. The magnitude of these
 970 quantities depends on the extent or size of the system (Cohen et al. 2008).

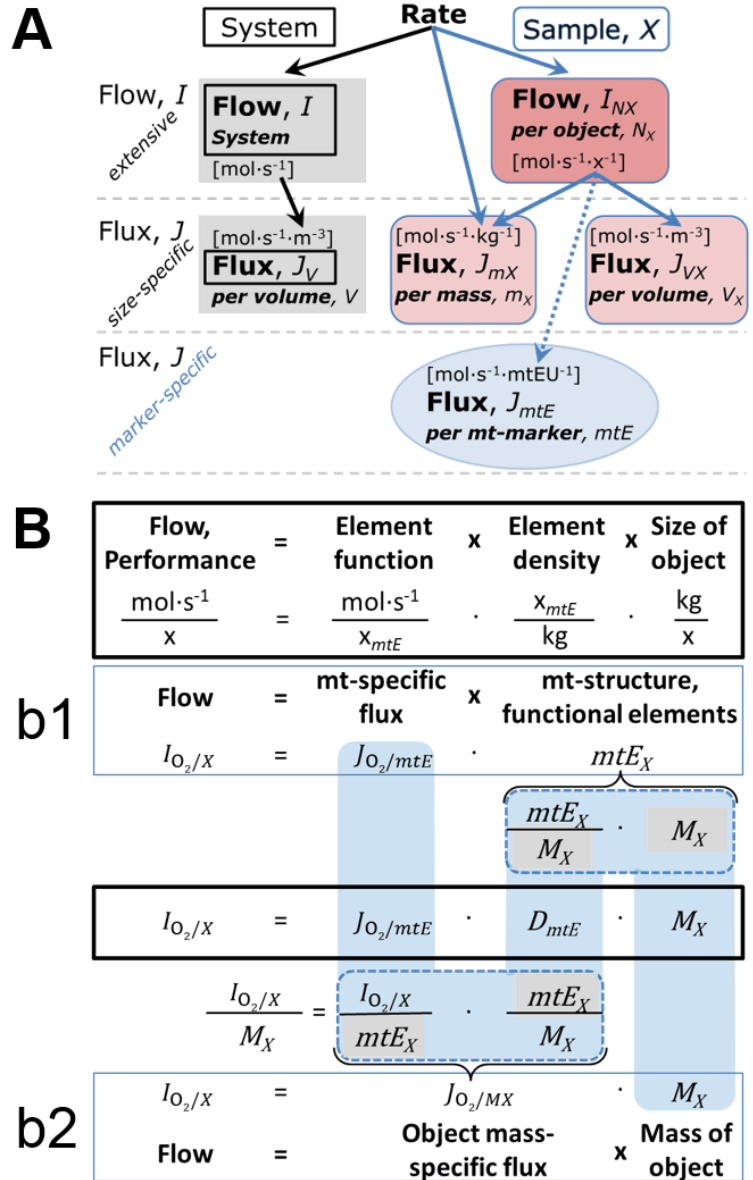
971 **Size-specific quantities:** ‘The adjective *specific* before the name of an extensive quantity
 972 is often used to mean *divided by mass*’ (Cohen et al. 2008). In this system-paradigm, mass-
 973 specific flux is flow divided by mass of the *system* (the total mass of everything within the

974 measuring chamber or reactor). A mass-specific quantity is independent of the extent of non-
 975 interacting homogenous subsystems. Tissue-specific quantities (related to the *sample* in
 976 contrast to the *system*) are of fundamental interest in the field of comparative mitochondrial
 977 physiology, where *specific* refers to the *type of the sample* rather than *mass of the system*. The
 978 term *specific*, therefore, must be clarified; *sample-specific*, e.g., muscle mass-specific
 979 normalization, is distinguished from *system-specific* quantities (mass or volume; **Figure 7**).

981 **Figure 7. Flow and flux, and normalization in structure-function analysis**

982 **(A)** Different meanings of rate may lead to confusion, if the normalization is not sufficiently
 983 specified. Results are frequently expressed as mass-specific *flux*,
 984 J_{mX} , per mg protein, dry or wet weight (mass). Cell volume, V_{cell} ,
 985 may be used for normalization (volume-specific flux, $J_{V\text{cell}}$),
 986 which must be clearly distinguished from flow per cell,
 987 $I_{N\text{cell}}$, or flux, J_V , expressed for methodological reasons per
 988 volume of the measurement system.

989 **(B)** O_2 flow, $I_{O_2/X}$, is the product of performance per functional
 990 element (element function, mitochondria-specific flux),
 991 element density (mitochondrial density, D_{mtE}), and size of entity X
 992 (mass, M_X). **(b1)** Structured analysis: performance is the
 993 product of mitochondrial *function* (mt-specific flux) and *structure*
 994 (functional elements; D_{mtE} times mass of X). **(b2)** Unstructured
 995 analysis: performance is the product of *entity mass-specific*
 996 *flux*, $J_{O_2/MX} = I_{O_2/X}/M_X = I_{O_2}/m_X$
 997 $[\text{mol}\cdot\text{s}^{-1}\cdot\text{kg}^{-1}]$ and *size of entity*, expressed as mass of X ; $M_X = m_X\cdot N_X^{-1}$ $[\text{kg}\cdot\text{x}^{-1}]$. Modified from
 998 Gnaiger (2014). For further details see **Table 4**.



1017 3.2. Normalization for system-size: flux per chamber volume

1018 **System-specific flux, J_{V,O_2} :** The experimental system (experimental chamber) is part of
 1019 the measurement apparatus, separated from the environment as an isolated, closed, open,
 1020 isothermal or non-isothermal system (**Table 4**). On another level, we distinguish between (1)
 1021 the *system* with volume V and mass m defined by the system boundaries, and (2) the *sample* or
 1022 *objects* with volume V_X and mass m_X that are enclosed in the experimental chamber (**Figure 7**).
 1023 Metabolic O_2 flow per object, $I_{O_2/X}$, increases as the mass of the object is increased. Sample
 1024

1025 mass-specific O₂ flux, $J_{O_2/mX}$ should be independent of the mass of the sample studied in the
 1026 instrument chamber, but system volume-specific O₂ flux, J_{V,O_2} (per volume of the instrument
 1027 chamber), should increase in direct proportion to the mass of the sample in the chamber.
 1028 Whereas J_{V,O_2} depends on mass-concentration of the sample in the chamber, it should be
 1029 independent of the chamber (system) volume at constant sample mass. There are practical
 1030 limitations to increase the mass-concentration of the sample in the chamber, when one is
 1031 concerned about crowding effects and instrumental time resolution.

1032 When the reactor volume does not change during the reaction, which is typical for liquid
 1033 phase reactions, the volume-specific flux of a chemical reaction r is the time derivative of the
 1034 advancement of the reaction per unit volume, $J_{V,rB} = d_r\zeta_B/dt \cdot V^{-1}$ [(mol·s⁻¹)·L⁻¹]. The rate of
 1035 concentration change is dc_B/dt [(mol·L⁻¹)·s⁻¹], where concentration is $c_B = n_B/V$. There is a
 1036 difference between (1) J_{V,rO_2} [mol·s⁻¹·L⁻¹] and (2) rate of concentration change [mol·L⁻¹·s⁻¹].
 1037 These merge to a single expression only in closed systems. In open systems, external fluxes
 1038 (such as O₂ supply) are distinguished from internal transformations (catabolic flux, O₂
 1039 consumption). In a closed system, external flows of all substances are zero and O₂ consumption
 1040 (internal flow of catabolic reactions k), I_{kO_2} [pmol·s⁻¹], causes a decline of the amount of O₂ in
 1041 the system, n_{O_2} [nmol]. Normalization of these quantities for the volume of the system, V [L \equiv
 1042 dm³], yields volume-specific O₂ flux, $J_{V,kO_2} = I_{kO_2}/V$ [nmol·s⁻¹·L⁻¹], and O₂ concentration, [O₂]
 1043 or $c_{O_2} = n_{O_2}/V$ [μ mol·L⁻¹ = μ M = nmol·mL⁻¹]. Instrumental background O₂ flux is due to external
 1044 flux into a non-ideal closed respirometer; then total volume-specific flux has to be corrected for
 1045 instrumental background O₂ flux—O₂ diffusion into or out of the instrumental chamber. J_{V,kO_2}
 1046 is relevant mainly for methodological reasons and should be compared with the accuracy of
 1047 instrumental resolution of background-corrected flux, e.g., ± 1 nmol·s⁻¹·L⁻¹ (Gnaiger 2001).
 1048 ‘Metabolic’ or catabolic indicates O₂ flux, J_{kO_2} , corrected for: (1) instrumental background O₂
 1049 flux; (2) chemical background O₂ flux due to autoxidation of chemical components added to
 1050 the incubation medium; and (3) Rox for O₂-consuming side reactions unrelated to the catabolic
 1051 pathway k .

1052 3.3. Normalization: per sample

1055 The challenges of measuring mitochondrial respiratory flux are matched by those of
 1056 normalization. Application of common and defined units is required for direct transfer of
 1057 reported results into a database. The second [s] is the SI unit for the base quantity *time*. It is also
 1058 the standard time-unit used in solution chemical kinetics. A rate may be considered as the
 1059 numerator and normalization as the complementary denominator, which are tightly linked in
 1060 reporting the measurements in a format commensurate with the requirements of a database.
 1061 Normalization (Table 4) is guided by physicochemical principles, methodological
 1062 considerations, and conceptual strategies (Figure 7).

1063 **Sample concentration, C_{mX} :** Normalization for sample concentration is required to
 1064 report respiratory data. Considering a tissue or cells as the sample, X , the sample mass is m_X
 1065 [mg], which is frequently measured as wet or dry weight, W_w or W_d [mg], respectively, or as
 1066 amount of tissue or cell protein, m_{Protein} . In the case of permeabilized tissues, cells, and
 1067 homogenates, the sample concentration, $C_{mX} = m_X/V$ [g·L⁻¹ = mg·mL⁻¹], is the mass of the
 1068 subsample of tissue that is transferred into the instrument chamber.

1069 **Mass-specific flux, $J_{O_2/mX}$:** Mass-specific flux is obtained by expressing respiration per
 1070 mass of sample, m_X [mg]. X is the type of sample—isolated mitochondria, tissue homogenate,
 1071 permeabilized fibres or cells. Volume-specific flux is divided by mass concentration of X , $J_{O_2/mX}$
 1072 = $J_{V,O_2}/C_{mX}$; or flow per cell is divided by mass per cell, $J_{O_2/mcell} = I_{O_2/cell}/M_{cell}$. If mass-specific
 1073 O₂ flux is constant and independent of sample size (expressed as mass), then there is no
 1074 interaction between the subsystems. A 1.5 mg and a 3.0 mg muscle sample respire at identical
 1075 mass-specific flux. Mass-specific O₂ flux, however, may change with the mass of a tissue

1076 sample, cells or isolated mitochondria in the measuring chamber, in which the nature of the
 1077 interaction becomes an issue. Therefore, cell density must be optimized, particularly in
 1078 experiments carried out in wells, considering the confluency of the cell monolayer or clumps
 1079 of cells (Salabei *et al.* 2014).

1080
 1081
 1082

Table 4. Sample concentrations and normalization of flux.

Expression	Symbol	Definition	Unit	Notes
Sample				
identity of sample	X	object: cell, tissue, animal, patient		
number of sample entities X	N_X	number of objects	x	
mass of sample X	m_X		kg	1
mass of object X	M_X	$M_X = m_X \cdot N_X^{-1}$	$\text{kg} \cdot \text{x}^{-1}$	1
Mitochondria				
mitochondria	mt	$X = \text{mt}$		
amount of mt-elements	mtE	quantity of mt-marker	mtEU	
Concentrations				
object number concentration	C_{NX}	$C_{NX} = N_X \cdot V^{-1}$	$\text{x} \cdot \text{m}^{-3}$	2
sample mass concentration	C_{mX}	$C_{mX} = m_X \cdot V^{-1}$	$\text{kg} \cdot \text{m}^{-3}$	
mitochondrial concentration	C_{mtE}	$C_{mtE} = mtE \cdot V^{-1}$	$\text{mtEU} \cdot \text{m}^{-3}$	3
specific mitochondrial density	D_{mtE}	$D_{mtE} = mtE \cdot m_X^{-1}$	$\text{mtEU} \cdot \text{kg}^{-1}$	4
mitochondrial content, mtE per object X	mtE_X	$mtE_X = mtE \cdot N_X^{-1}$	$\text{mtEU} \cdot \text{x}^{-1}$	5
O₂ flow and flux				
flow, system	I_{O_2}	internal flow	$\text{mol} \cdot \text{s}^{-1}$	6
volume-specific flux	J_{V,O_2}	$J_{V,O_2} = I_{O_2} \cdot V^{-1}$	$\text{mol} \cdot \text{s}^{-1} \cdot \text{m}^{-3}$	7
flow per object X	$I_{O_2/X}$	$I_{O_2/X} = J_{V,O_2} \cdot C_{NX}^{-1}$	$\text{mol} \cdot \text{s}^{-1} \cdot \text{x}^{-1}$	8
mass-specific flux	$J_{O_2/mX}$	$J_{O_2/mX} = J_{V,O_2} \cdot C_{mX}^{-1}$	$\text{mol} \cdot \text{s}^{-1} \cdot \text{kg}^{-1}$	9
mitochondria-specific flux	$J_{O_2/mtE}$	$J_{O_2/mtE} = J_{V,O_2} \cdot C_{mtE}^{-1}$	$\text{mol} \cdot \text{s}^{-1} \cdot \text{mtEU}^{-1}$	10

- 1083 1 Units are given in the MKSA system (**Box 2**). The *SI* prefix k is used for the *SI* base unit of mass (kg
 1084 = 1,000 g). In praxis, various *SI* prefixes are used for convenience, to make numbers easily readable,
 1085 e.g., 1 mg tissue, cell or mitochondrial mass instead of 0.000001 kg.
- 1086 2 In case sample $X = \text{cells}$, the object number concentration is $C_{N_{\text{cell}}} = N_{\text{cell}} \cdot V^{-1}$, and volume may be
 1087 expressed in [$\text{dm}^3 \equiv \text{L}$] or [$\text{cm}^3 = \text{mL}$]. See **Table 5** for different object types.
- 1088 3 mt-concentration is an experimental variable, dependent on sample concentration: (1) $C_{mtE} = mtE \cdot V^{-1}$;
 1089 (2) $C_{mtE} = mtE_X \cdot C_{NX}$; (3) $C_{mtE} = C_{mX} \cdot D_{mtE}$.
- 1090 4 If the amount of mitochondria, mtE , is expressed as mitochondrial mass, then D_{mtE} is the mass
 1091 fraction of mitochondria in the sample. If mtE is expressed as mitochondrial volume, V_{mt} , and the
 1092 mass of sample, m_X , is replaced by volume of sample, V_X , then D_{mtE} is the volume fraction of
 1093 mitochondria in the sample.
- 1094 5 $mtE_X = mtE \cdot N_X^{-1} = C_{mtE} \cdot C_{NX}^{-1}$.
- 1095 6 O₂ can be replaced by other chemicals B to study different reactions, e.g., ATP, H₂O₂, or vesicular
 1096 compartmental translocations, e.g., Ca²⁺.
- 1097 7 I_{O_2} and V are defined per instrument chamber as a system of constant volume (and constant
 1098 temperature), which may be closed or open. I_{O_2} is abbreviated for I_{r,O_2} , i.e., the metabolic or internal
 1099 O₂ flow of the chemical reaction r in which O₂ is consumed, hence the negative stoichiometric
 1100 number, $\nu_{O_2} = -1$. $I_{r,O_2} = d_r n_{O_2} / dt \cdot \nu_{O_2}^{-1}$. If r includes all chemical reactions in which O₂ participates, then
 1101 $d_r n_{O_2} = dn_{O_2} - d_e n_{O_2}$, where dn_{O_2} is the change in the amount of O₂ in the instrument chamber and $d_e n_{O_2}$
 1102 is the amount of O₂ added externally to the system. At steady state, by definition $dn_{O_2} = 0$, hence $d_r n_{O_2}$
 1103 = $-d_e n_{O_2}$.

- 1104 8 J_{V,O_2} is an experimental variable, expressed per volume of the instrument chamber.
 1105 9 $I_{O_2/X}$ is a physiological variable, depending on the size of entity X .
 1106 10 There are many ways to normalize for a mitochondrial marker, that are used in different experimental
 1107 approaches: (1) $J_{O_2/mtE} = J_{V,O_2} \cdot C_{mtE}^{-1}$; (2) $J_{O_2/mtE} = J_{V,O_2} \cdot C_{mX}^{-1} \cdot D_{mtE}^{-1} = J_{O_2/mX} \cdot D_{mtE}^{-1}$; (3) $J_{O_2/mtE} =$
 1108 $J_{V,O_2} \cdot C_{NX}^{-1} \cdot mtE_X^{-1} = I_{O_2/X} \cdot mtE_X^{-1}$; (4) $J_{O_2/mtE} = I_{O_2} \cdot mtE^{-1}$. The mt-elemental unit [mtEU] varies between
 1109 different mt-markers.
 1110
 1111

1112 **Number concentration, C_{NX} :** C_{NX} is the experimental *number concentration* of sample
 1113 X . In the case of cells or animals, e.g., nematodes, $C_{NX} = N_X/V [X \cdot L^{-1}]$, where N_X is the number
 1114 of cells or organisms in the chamber (**Table 4**).

1115 **Flow per object, $I_{O_2/X}$:** A special case of normalization is encountered in respiratory
 1116 studies with permeabilized (or intact) cells. If respiration is expressed per cell, the O_2 flow per
 1117 measurement system is replaced by the O_2 flow per cell, $I_{O_2/cell}$ (**Table 4**). O_2 flow can be
 1118 calculated from volume-specific O_2 flux, $J_{V,O_2} [nmol \cdot s^{-1} \cdot L^{-1}]$ (per V of the measurement chamber
 1119 [L]), divided by the number concentration of cells, $C_{N_{cell}} = N_{cell}/V [cell \cdot L^{-1}]$, where N_{cell} is the
 1120 number of cells in the chamber. The total cell count is the sum of viable and dead cells, $N_{cell} =$
 1121 $N_{vce} + N_{dce}$ (**Table 5**). The cell viability index, $CVI = N_{vce}/N_{cell}$, is the ratio of viable cells (N_{vce} ;
 1122 before experimental permeabilization) per total cell count. After experimental permeabilization,
 1123 all cells are permeabilized, $N_{pce} = N_{cell}$. The cell viability index can be used to normalize
 1124 respiration for the number of cells that have been viable before experimental permeabilization,
 1125 $I_{O_2/vce} = I_{O_2/cell}/CVI$, considering that mitochondrial respiratory dysfunction in dead cells should
 1126 be eliminated as a confounding factor.
 1127

1128 **Table 5. Sample types, X , abbreviations, and quantification.**

Identity of sample	X	N_X	Mass ^a	Volume	mt-Marker
mitochondrial preparation	mt-prep	[x]	[kg]	[m ³]	[mtEU]
isolated mitochondria	imt		m_{mt}	V_{mt}	mtE
tissue homogenate	thom		m_{thom}		mtE_{thom}
permeabilized tissue	pti		m_{pti}		mtE_{pti}
permeabilized fibre	pfi		m_{pfi}		mtE_{pfi}
permeabilized cell	pce	N_{pce}	M_{pce}	V_{pce}	mtE_{pce}
cells ^b	cell	N_{cell}	M_{cell}	V_{cell}	mtE_{cell}
intact cell, viable cell	vce	N_{vce}	M_{vce}	V_{vce}	
dead cell	dce	N_{dce}	M_{dce}	V_{dce}	
organism	org	N_{org}	M_{org}	V_{org}	

1129 ^a Instead of mass, the wet weight or dry weight is frequently stated, W_w or W_d .

1130 m_X is mass of the sample [kg], M_X is mass of the object [kg·x⁻¹].

1131 ^b Total cell count, $N_{cell} = N_{vce} + N_{dce}$
 1132

1133 Cellular O_2 flow can be compared between cells of identical size. To take into account
 1134 changes and differences in cell size, normalization is required to obtain cell size-specific or
 1135 mitochondrial marker-specific O_2 flux (Renner *et al.* 2003).

1136 The complexity changes when the sample is a whole organism studied as an experimental
 1137 model. The scaling law in respiratory physiology reveals a strong interaction of O_2 flow and
 1138 individual body mass of an organism, since *basal* metabolic rate (flow) does not increase
 1139 linearly with body mass, whereas *maximum* mass-specific O_2 flux, \dot{V}_{O_2max} or \dot{V}_{O_2peak} , is
 1140 approximately constant across a large range of individual body mass (Weibel and Hoppeler
 1141 2005), with individuals, breeds, and species deviating substantially from this relationship.

1142 $\dot{V}O_{2peak}$ of human endurance athletes is 60 to 80 mL O₂·min⁻¹·kg⁻¹ body mass, converted to
 1143 $J_{O_{2peak}/M}$ of 45 to 60 nmol·s⁻¹·g⁻¹ (Gnaiger 2014; **Table 6**).

1144 3.4. Normalization for mitochondrial content

1145

1146 Tissues can contain multiple cell populations that may have distinct mitochondrial
 1147 subtypes. Mitochondria undergo dynamic fission and fusion cycles, and can exist in multiple
 1148 stages and sizes that may be altered by a range of factors. The isolation of mitochondria (often
 1149 achieved through differential centrifugation) can therefore yield a subsample of the
 1150 mitochondrial types present in a tissue, depending on the isolation protocols utilized (*e.g.*,
 1151 centrifugation speed). This possible bias should be taken into account when planning
 1152 experiments using isolated mitochondria. Different sizes of mitochondria are enriched at
 1153 specific centrifugation speeds, which can be used strategically for isolation of mitochondrial
 1154 subpopulations.

1155 Part of the mitochondrial content of a tissue is lost during preparation of isolated
 1156 mitochondria. The fraction of isolated mitochondria obtained from a tissue sample is expressed
 1157 as mitochondrial recovery. At a high mitochondrial recovery the fraction of isolated
 1158 mitochondria is more representative of the total mitochondrial population than in preparations
 1159 characterized by low recovery. Determination of the mitochondrial recovery and yield is based
 1160 on measurement of the concentration of a mitochondrial marker in the stock of isolated
 1161 mitochondria, $C_{mtE,stock}$, and crude tissue homogenate, $C_{mtE,thom}$, which simultaneously provides
 1162 information on the specific mitochondrial density in the sample, D_{mtE} (**Table 4**).

1163 Normalization is a problematic subject; it is essential to consider the question of the study.
 1164 If the study aims at comparing tissue performance—such as the effects of a treatment on a
 1165 specific tissue, then normalization for tissue mass or protein content is appropriate. However,
 1166 if the aim is to find differences on mitochondrial function independent of mitochondrial density
 1167 (**Table 4**), then normalization to a mitochondrial marker is imperative (**Figure 7**). One cannot
 1168 assume that quantitative changes in various markers—such as mitochondrial proteins—
 1169 necessarily occur in parallel with one another. It should be established that the marker chosen
 1170 is not selectively altered by the performed treatment. In conclusion, the normalization must
 1171 reflect the question under investigation to reach a satisfying answer. On the other hand, the goal
 1172 of comparing results across projects and institutions requires standardization on normalization
 1173 for entry into a databank.

1174 **Mitochondrial concentration, C_{mtE} , and mitochondrial markers:** Mitochondrial
 1175 organelles comprise a dynamic cellular reticulum in various states of fusion and fission. Hence,
 1176 the definition of an "amount" of mitochondria is often misconceived: mitochondria cannot be
 1177 counted reliably as a number of occurring elements. Therefore, quantification of the "amount"
 1178 of mitochondria depends on the measurement of chosen mitochondrial markers. 'Mitochondria
 1179 are the structural and functional elemental units of cell respiration' (Gnaiger 2014). The
 1180 quantity of a mitochondrial marker can reflect the amount of *mitochondrial elements*, mtE ,
 1181 expressed in various mitochondrial elemental units [mtEU] specific for each measured mt-
 1182 marker (**Table 4**). However, since mitochondrial quality may change in response to stimuli—
 1183 particularly in mitochondrial dysfunction and after exercise training (Pesta *et al.* 2011; Campos
 1184 *et al.* 2017)—some markers can vary while others are unchanged: (1) Mitochondrial volume
 1185 and membrane area are structural markers, whereas mitochondrial protein mass is frequently
 1186 used as a marker for isolated mitochondria. (2) Molecular and enzymatic mitochondrial markers
 1187 (amounts or activities) can be selected as matrix markers, *e.g.*, citrate synthase activity, mtDNA;
 1188 mtIM-markers, *e.g.*, cytochrome *c* oxidase activity, *aa₃* content, cardiolipin, or mtOM-markers,
 1189 *e.g.*, TOM20. (3) Extending the measurement of mitochondrial marker enzyme activity to
 1190 mitochondrial pathway capacity, ET- or OXPHOS-capacity can be considered as an integrative
 1191 functional mitochondrial marker.

1192 Depending on the type of mitochondrial marker, the mitochondrial elements, mtE , are
 1193 expressed in marker-specific units. Mitochondrial concentration in the measurement chamber
 1194 and the tissue of origin are quantified as (1) a quantity for normalization in functional analyses,
 1195 C_{mtE} , and (2) a physiological output that is the result of mitochondrial biogenesis and
 1196 degradation, D_{mtE} , respectively (Table 4). It is recommended, therefore, to distinguish
 1197 *experimental mitochondrial concentration*, $C_{mtE} = mtE/V$ and *physiological mitochondrial*
 1198 *density*, $D_{mtE} = mtE/m_X$. Then mitochondrial density is the amount of mitochondrial elements
 1199 per mass of tissue, which is a biological variable (Figure 7). The experimental variable is
 1200 mitochondrial density multiplied by sample mass concentration in the measuring chamber, C_{mtE}
 1201 $= D_{mtE} \cdot C_{mX}$, or mitochondrial content multiplied by sample number concentration, $C_{mtE} =$
 1202 $mtE_X \cdot C_{NX}$ (Table 4).

1203 **Mitochondria-specific flux, $J_{O_2/mtE}$:** Volume-specific metabolic O_2 flux depends on: (1)
 1204 the sample concentration in the volume of the instrument chamber, C_{mX} , or C_{NX} ; (2) the
 1205 mitochondrial density in the sample, $D_{mtE} = mtE/m_X$ or $mtE_X = mtE/N_X$; and (3) the specific
 1206 mitochondrial activity or performance per elemental mitochondrial unit, $J_{O_2/mtE} = J_{V,O_2}/C_{mtE}$
 1207 $[\text{mol}\cdot\text{s}^{-1}\cdot\text{mtEU}^{-1}]$ (Table 4). Obviously, the numerical results for $J_{O_2/mtE}$ vary with the type of
 1208 mitochondrial marker chosen for measurement of mtE and $C_{mtE} = mtE/V$ $[\text{mtEU}\cdot\text{m}^{-3}]$.
 1209

1210 3.5. Evaluation of mitochondrial markers

1211
 1212 Different methods are implicated in the quantification of mitochondrial markers and have
 1213 different strengths. Some problems are common for all mitochondrial markers, mtE : (1)
 1214 Accuracy of measurement is crucial, since even a highly accurate and reproducible
 1215 measurement of O_2 flux results in an inaccurate and noisy expression if normalized by a biased
 1216 and noisy measurement of a mitochondrial marker. This problem is acute in mitochondrial
 1217 respiration because the denominators used (the mitochondrial markers) are often small moieties
 1218 of which accurate and precise determination is difficult. This problem can be avoided when O_2
 1219 fluxes measured in substrate-uncoupler-inhibitor titration protocols are normalized for flux in
 1220 a defined respiratory reference state, which is used as an *internal* marker and yields flux control
 1221 ratios, *FCRs*. *FCRs* are independent of *externally* measured markers and, therefore, are
 1222 statistically robust, considering the limitations of ratios in general (Jasienski and Bazzaz 1999).
 1223 *FCRs* indicate qualitative changes of mitochondrial respiratory control, with highest
 1224 quantitative resolution, separating the effect of mitochondrial density or concentration on $J_{O_2/mX}$
 1225 and $I_{O_2/X}$ from that of function per elemental mitochondrial marker, $J_{O_2/mtE}$ (Pesta *et al.* 2011;
 1226 Gnaiger 2014). (2) If mitochondrial quality does not change and only the amount of
 1227 mitochondria varies as a determinant of mass-specific flux, any marker is equally qualified in
 1228 principle; then in practice selection of the optimum marker depends only on the accuracy and
 1229 precision of measurement of the mitochondrial marker. (3) If mitochondrial flux control ratios
 1230 change, then there may not be any best mitochondrial marker. In general, measurement of
 1231 multiple mitochondrial markers enables a comparison and evaluation of normalization for a
 1232 variety of mitochondrial markers. Particularly during postnatal development, the activity of
 1233 marker enzymes—such as cytochrome *c* oxidase and citrate synthase—follows different time
 1234 courses (Drahota *et al.* 2004). Evaluation of mitochondrial markers in healthy controls is
 1235 insufficient for providing guidelines for application in the diagnosis of pathological states and
 1236 specific treatments.

1237 In line with the concept of the respiratory control ratio (Chance and Williams 1955a), the
 1238 most readily used normalization is that of flux control ratios and flux control factors (Gnaiger
 1239 2014). Selection of the state of maximum flux in a protocol as the reference state has the
 1240 advantages of: (1) internal normalization; (2) statistical linearization of the response in the range
 1241 of 0 to 1; and (3) consideration of maximum flux for integrating a large number of elemental
 1242 steps in the OXPHOS- or ET-pathways. This reduces the risk of selecting a functional marker

1243 that is specifically altered by the treatment or pathology, yet increases the chance that the highly
 1244 integrative pathway is disproportionately affected, *e.g.*, the OXPHOS- rather than ET-pathway
 1245 in case of an enzymatic defect in the phosphorylation-pathway. In this case, additional
 1246 information can be obtained by reporting flux control ratios based on a reference state which
 1247 indicates stable tissue-mass specific flux. Stereological determination of mitochondrial content
 1248 via two-dimensional transmission electron microscopy can have limitations due to the dynamics
 1249 of mitochondrial size (Meinild Lundby *et al.* 2017). Accurate determination of three-
 1250 dimensional volume by two-dimensional microscopy can be both time consuming and
 1251 statistically challenging (Larsen *et al.* 2012).

1252 The validity of using mitochondrial marker enzymes (citrate synthase activity, Complex
 1253 I–IV amount or activity) for normalization of flux is limited in part by the same factors that
 1254 apply to flux control ratios. Strong correlations between various mitochondrial markers and
 1255 citrate synthase activity (Reichmann *et al.* 1985; Boushel *et al.* 2007; Mogensen *et al.* 2007)
 1256 are expected in a specific tissue of healthy subjects and in disease states not specifically
 1257 targeting citrate synthase. Citrate synthase activity is acutely modifiable by exercise
 1258 (Tonkonogi *et al.* 1997; Leek *et al.* 2001). Evaluation of mitochondrial markers related to a
 1259 selected age and sex cohort cannot be extrapolated to provide recommendations for
 1260 normalization in respirometric diagnosis of disease, in different states of development and
 1261 ageing, different cell types, tissues, and species. mtDNA normalized to nDNA via qPCR is
 1262 correlated to functional mitochondrial markers including OXPHOS- and ET-capacity in some
 1263 cases (Puntschart *et al.* 1995; Wang *et al.* 1999; Menshikova *et al.* 2006; Boushel *et al.* 2007),
 1264 but lack of such correlations have been reported (Menshikova *et al.* 2005; Schultz and Wiesner
 1265 2000; Pesta *et al.* 2011). Several studies indicate a strong correlation between cardiolipin
 1266 content and increase in mitochondrial function with exercise (Menshikova *et al.* 2005;
 1267 Menshikova *et al.* 2007; Larsen *et al.* 2012; Faber *et al.* 2014), but it has not been evaluated as
 1268 a general mitochondrial biomarker in disease.

1269

1270 3.6. Conversion: units

1271

1272 Many different units have been used to report the O₂ consumption rate, OCR (**Table 6**).
 1273 *SI* base units provide the common reference to introduce the theoretical principles (**Figure 7**),
 1274 and are used with appropriately chosen *SI* prefixes to express numerical data in the most
 1275 practical format, with an effort towards unification within specific areas of application (**Table**
 1276 **7**). Reporting data in *SI* units—including the mole [mol], coulomb [C], joule [J], and second
 1277 [s]—should be encouraged, particularly by journals which propose the use of *SI* units.

1278 Although volume is expressed as m³ using the *SI* base unit, the litre [dm³] is a
 1279 conventional unit of volume for concentration and is used for most solution chemical kinetics.
 1280 If one multiplies $I_{O_2/cell}$ by C_{Ncell} , then the result will not only be the amount of O₂ [mol]
 1281 consumed per time [s⁻¹] in one litre [L⁻¹], but also the change in O₂ concentration per second
 1282 (for any volume of an ideally closed system). This is ideal for kinetic modeling as it blends with
 1283 chemical rate equations where concentrations are typically expressed in mol·L⁻¹ (Wagner *et al.*
 1284 2011). In studies of multinuclear cells—such as differentiated skeletal muscle cells—it is easy
 1285 to determine the number of nuclei but not the total number of cells. A generalized concept,
 1286 therefore, is obtained by substituting cells by nuclei as the sample entity. This does not hold,
 1287 however, for enucleated platelets.

1288 For studies of cells, we recommend that respiration be expressed, as far as possible, as:
 1289 (1) O₂ flux normalized for a mitochondrial marker, for separation of the effects of mitochondrial
 1290 quality and content on cell respiration (this includes *FCRs* as a normalization for a functional
 1291 mitochondrial marker); (2) O₂ flux in units of cell volume or mass, for comparison of respiration
 1292 of cells with different cell size (Renner *et al.* 2003) and with studies on tissue preparations, and
 1293 (3) O₂ flow in units of attomole (10⁻¹⁸ mol) of O₂ consumed in a second by each cell

1294 [amol·s⁻¹·cell⁻¹], numerically equivalent to [pmol·s⁻¹·10⁻⁶ cells]. This convention allows
 1295 information to be easily used when designing experiments in which O₂ flow must be considered.
 1296 For example, to estimate the volume-specific O₂ flux in an instrument chamber that would be
 1297 expected at a particular cell number concentration, one simply needs to multiply the flow per
 1298 cell by the number of cells per volume of interest. This provides the amount of O₂ [mol]
 1299 consumed per time [s⁻¹] per unit volume [L⁻¹]. At an O₂ flow of 100 amol·s⁻¹·cell⁻¹ and a cell
 1300 density of 10⁹ cells·L⁻¹ (10⁶ cells·mL⁻¹), the volume-specific O₂ flux is 100 nmol·s⁻¹·L⁻¹ (100
 1301 pmol·s⁻¹·mL⁻¹).

1303 **Table 6. Conversion of various units used in respirometry and**
 1304 **ergometry.** e⁻ is the number of electrons or reducing equivalents. z_B is the
 1305 charge number of entity B.
 1306

1 Unit		Multiplication factor	SI-unit	Note
ng.atom O·s ⁻¹	(2 e ⁻)	0.5	nmol O ₂ ·s ⁻¹	
ng.atom O·min ⁻¹	(2 e ⁻)	8.33	pmol O ₂ ·s ⁻¹	
natom O·min ⁻¹	(2 e ⁻)	8.33	pmol O ₂ ·s ⁻¹	
nmol O ₂ ·min ⁻¹	(4 e ⁻)	16.67	pmol O ₂ ·s ⁻¹	
nmol O ₂ ·h ⁻¹	(4 e ⁻)	0.2778	pmol O ₂ ·s ⁻¹	
mL O ₂ ·min ⁻¹ at STPD ^a		0.744	μmol O ₂ ·s ⁻¹	1
W = J/s at -470 kJ/mol O ₂		-2.128	μmol O ₂ ·s ⁻¹	
mA = mC·s ⁻¹	(z _{H+} = 1)	10.36	nmol H ⁺ ·s ⁻¹	2
mA = mC·s ⁻¹	(z _{O₂} = 4)	2.59	nmol O ₂ ·s ⁻¹	2
nmol H ⁺ ·s ⁻¹	(z _{H+} = 1)	0.09649	mA	3
nmol O ₂ ·s ⁻¹	(z _{O₂} = 4)	0.38594	mA	3

1307 1 At standard temperature and pressure dry (STPD: 0 °C = 273.15 K and 1 atm =
 1308 101.325 kPa = 760 mmHg), the molar volume of an ideal gas, V_m, and V_{m,O₂} is
 1309 22.414 and 22.392 L·mol⁻¹, respectively. Rounded to three decimal places, both
 1310 values yield the conversion factor of 0.744. For comparison at normal
 1311 temperature and pressure dry (NTPD: 20 °C), V_{m,O₂} is 24.038 L·mol⁻¹. Note that
 1312 the SI standard pressure is 100 kPa.

1313 2 The multiplication factor is 10⁶/(z_B·F).

1314 3 The multiplication factor is z_B·F/10⁶.

1315

1316 ET-capacity in human cell types including HEK 293, primary HUVEC and fibroblasts
 1317 ranges from 50 to 180 amol·s⁻¹·cell⁻¹, measured in intact cells in the noncoupled state (see
 1318 Gnaiger 2014). At 100 amol·s⁻¹·cell⁻¹ corrected for *Rox*, the current across the mt-membranes,
 1319 I_{H⁺e⁻}, approximates 193 pA·cell⁻¹ or 0.2 nA per cell. See Rich (2003) for an extension of
 1320 quantitative bioenergetics from the molecular to the human scale, with a transmembrane proton
 1321 flux equivalent to 520 A in an adult at a catabolic power of -110 W. Modelling approaches
 1322 illustrate the link between protonmotive force and currents (Willis *et al.* 2016).

1323 We consider isolated mitochondria as powerhouses and proton pumps as molecular
 1324 machines to relate experimental results to energy metabolism of the intact cell. The cellular
 1325 P_»/O₂ based on oxidation of glycogen is increased by the glycolytic (fermentative) substrate-
 1326 level phosphorylation of 3 P_»/Glyc or 0.5 mol P_» for each mol O₂ consumed in the complete
 1327 oxidation of a mol glycosyl unit (Glyc). Adding 0.5 to the mitochondrial P_»/O₂ ratio of 5.4
 1328 yields a bioenergetic cell physiological P_»/O₂ ratio close to 6. Two NADH equivalents are
 1329 formed during glycolysis and transported from the cytosol into the mitochondrial matrix, either
 1330 by the malate-aspartate shuttle or by the glycerophosphate shuttle (**Figure 2A**) resulting in

1331 different theoretical yields of ATP generated by mitochondria, the energetic cost of which
 1332 potentially must be taken into account. Considering also substrate-level phosphorylation in the
 1333 TCA cycle, this high P_{\gg}/O_2 ratio not only reflects proton translocation and OXPHOS studied
 1334 in isolation, but integrates mitochondrial physiology with energy transformation in the living
 1335 cell (Gnaiger 1993a).

1336
 1337

Table 7. Conversion of units with preservation of numerical values.

Name	Frequently used unit	Equivalent unit	Note
volume-specific flux, J_{V,O_2}	$\text{pmol}\cdot\text{s}^{-1}\cdot\text{mL}^{-1}$ $\text{mmol}\cdot\text{s}^{-1}\cdot\text{L}^{-1}$	$\text{nmol}\cdot\text{s}^{-1}\cdot\text{L}^{-1}$ $\text{mol}\cdot\text{s}^{-1}\cdot\text{m}^{-3}$	1
cell-specific flow, $I_{O_2/\text{cell}}$	$\text{pmol}\cdot\text{s}^{-1}\cdot 10^{-6}$ cells	$\text{amol}\cdot\text{s}^{-1}\cdot\text{cell}^{-1}$	2
	$\text{pmol}\cdot\text{s}^{-1}\cdot 10^{-9}$ cells	$\text{zmol}\cdot\text{s}^{-1}\cdot\text{cell}^{-1}$	3
cell number concentration, C_{Nce}	10^6 cells $\cdot\text{mL}^{-1}$	10^9 cells $\cdot\text{L}^{-1}$	
mitochondrial protein concentration, C_{mtE}	0.1 mg $\cdot\text{mL}^{-1}$	0.1 g $\cdot\text{L}^{-1}$	
mass-specific flux, $J_{O_2/m}$	$\text{pmol}\cdot\text{s}^{-1}\cdot\text{mg}^{-1}$	$\text{nmol}\cdot\text{s}^{-1}\cdot\text{g}^{-1}$	4
catabolic power, P_k	$\mu\text{W}\cdot 10^{-6}$ cells	$\text{pW}\cdot\text{cell}^{-1}$	1
volume	1,000 L	m^3 (1,000 kg)	
	L	dm^3 (kg)	
	mL	cm^3 (g)	
	μL	mm^3 (mg)	
	fL	μm^3 (pg)	5
amount of substance concentration	$\text{M} = \text{mol}\cdot\text{L}^{-1}$	$\text{mol}\cdot\text{dm}^{-3}$	

1338

1339 1 pmol: picomole = 10^{-12} mol

1340 2 amol: attomole = 10^{-18} mol

1341 3 zmol: zeptomole = 10^{-21} mol

1342

1343

1344 4. Conclusions

1345

1346 MitoEAGLE can serve as a gateway to better diagnose mitochondrial respiratory defects
 1347 linked to genetic variation, age-related health risks, sex-specific mitochondrial performance,
 1348 lifestyle with its effects on degenerative diseases, and thermal and chemical environment. The
 1349 present recommendations on coupling control states and rates, linked to the concept of the
 1350 protonmotive force, are focused on studies with mitochondrial preparations. These will be
 1351 extended in a series of reports on pathway control of mitochondrial respiration, respiratory
 1352 states in intact cells, and harmonization of experimental procedures.

1353 OXPHOS analysis is based on the study of mitochondrial preparations complementary to
 1354 bioenergetic investigations of intact cells and organisms—from animal models to healthy
 1355 persons or patients. Metabolic fluxes measured in defined coupling and pathway control states
 1356 provide insights into the meaning of cellular and organismic respiration. An O_2 flux balance
 1357 scheme illustrates the relationships and general definitions (**Figures 1 and 2**).

1358 Catabolic cell respiration is the process of exergonic and exothermic energy
 1359 transformation in which scalar redox reactions are coupled to vectorial ion translocation across
 1360 a semipermeable membrane, which separates the small volume of a bacterial cell or
 1361 mitochondrion from the larger volume of its surroundings. The electrochemical exergy can be
 1362 partially conserved in the phosphorylation of ADP to ATP or in ion pumping, or dissipated in
 1363 an electrochemical short-circuit. Respiration is thus clearly distinguished from fermentation as

1364 the counterpart of cellular core energy metabolism. Respiration is separated in mitochondrial
1365 preparations from the interactions with the fermentative pathways of the intact cell.

1366 The optimal choice for expressing mitochondrial and cell respiration as O₂ flow per
1367 biological sample, and normalization for specific tissue-markers (volume, mass, protein) and
1368 mitochondrial markers (volume, protein, content, mtDNA, activity of marker enzymes,
1369 respiratory reference state) is guided by the scientific question under study. Interpretation of
1370 the data depends critically on appropriate normalization.

1371 We recommend for studies with mitochondrial preparations:

1372 • Normalization of respiratory rates should be provided as far as possible:

1373 1. Biophysical normalization: on a per cell basis as O₂ flow; this may not be possible
1374 when dealing with tissues

1375 2. Cellular normalization: per g protein; per cell- or tissue-mass as mass-specific O₂
1376 flux; per cell volume as cell volume-specific flux

1377 3. Mitochondrial normalization: per mitochondrial marker as mt-specific flux.

1378 With information on cell size and the use of multiple normalizations, maximum potential
1379 information is available (Renner *et al.* 2003; Wagner *et al.* 2011; Gnaiger 2014).
1380 Reporting flow in a respiratory chamber [nmol·s⁻¹] is discouraged, since it restricts the
1381 analysis to intra-experimental comparison of relative (qualitative) differences.

1382 • Catabolic mitochondrial respiration is distinguished from residual oxygen consumption.
1383 Fluxes in mitochondrial coupling states should be, as far as possible, corrected for residual
1384 oxygen consumption.

1385 • Different mechanisms of uncoupling should be distinguished by defined terms. The
1386 tightness of coupling relates to these uncoupling mechanisms, whereas the coupling
1387 stoichiometry varies as a function the substrate type involved in ET-pathways with either
1388 three or two redox proton pumps operating in series. Separation of tightness of coupling
1389 from the pathway-dependent coupling stoichiometry is possible only when the substrate
1390 type undergoing oxidation remains the same for respiration in LEAK-, OXPHOS-, and
1391 ET-states. In studies of the tightness of coupling, therefore, simple substrate-inhibitor
1392 combinations should be applied to exclude a shift in substrate competition which may
1393 occur when providing physiological substrate cocktails.

1394 • In studies of isolated mitochondria, the mitochondrial recovery and yield should be
1395 reported. Experimental criteria for evaluation of purity versus integrity should be
1396 considered. Mitochondrial markers—such as citrate synthase activity as an enzymatic
1397 matrix marker—provide a link to the tissue of origin on the basis of calculating the
1398 mitochondrial recovery, *i.e.*, the fraction of mitochondrial marker obtained from a unit
1399 mass of tissue. Total mitochondrial protein is frequently applied as a mitochondrial
1400 marker, which is restricted to isolated mitochondria.

1401 • In studies of permeabilized cells, the viability of the cell culture or cell suspension of
1402 origin should be reported. Normalization should be evaluated for total cell count or viable
1403 cell count.

1404 • Terms and symbols are summarized in **Table 8**. Their use will facilitate transdisciplinary
1405 communication and support further developments towards a consistent theory of
1406 bioenergetics and mitochondrial physiology. Technical terms related to and defined with
1407 normal words can be used as index terms in databases, support the creation of ontologies
1408 towards semantic information processing (MitoPedia), and help in communicating
1409 analytical findings as impactful data-driven stories. ‘*Making data available without
1410 making it understandable may be worse than not making it available at all*’ (National
1411 Academies of Sciences, Engineering, and Medicine 2018). Success will depend on taking
1412 next steps: (1) exhaustive text-mining considering Omics data and functional data; (2)
1413 network analysis of Omics data with bioinformatics tools; (3) cross-validation with
1414 distinct bioinformatics approaches; (4) correlation with functional data; (5) guidelines for

1415 biological validation of network data. This is a call to carefully contribute to FAIR
 1416 principles (Findable, Accessible, Interoperable, Reusable) for the sharing of scientific
 1417 data.
 1418

1419 **Table 8. Terms, symbols, and units.**
 1420
 1421

1422 Term	1423 Symbol	1424 Unit	1425 Links and comments
1426 alternative quinol oxidase	1427 AOX		1428 Figure 2B
1429 amount of substance B	1430 n_B	1431 [mol]	
1432 ATP yield per O_2	1433 Y_{P_{\gg}/O_2}		1434 P_{\gg}/O_2 ratio measured in any respiratory 1435 state
1436 catabolic reaction	1437 k		1438 Figure 1 and 3
1439 catabolic respiration	1440 J_{kO_2}	1441 <i>varies</i>	1442 Figure 1 and 3
1443 cell number	1444 N_{cell}	1445 [x]	1446 Table 5; $N_{\text{cell}} = N_{\text{vce}} + N_{\text{dce}}$
1447 cell respiration	1448 J_{rO_2}	1449 <i>varies</i>	1450 Figure 1
1451 cell viability index	1452 CVI		1453 $CVI = N_{\text{vce}}/N_{\text{cell}} = 1 - N_{\text{dce}}/N_{\text{cell}}$
1454 Complexes I to IV	1455 CI to CIV		1456 respiratory ET Complexes; Figure 2B
1457 concentration of substance B	1458 $c_B = n_B \cdot V^{-1}$; [B]	1459 [mol·m ⁻³]	1460 Box 2
1461 dead cell number	1462 N_{dce}	1463 [x]	1464 Table 5; non-viable cells, loss of plasma 1465 membrane barrier function
1466 electron transfer system	1467 ETS		1468 Figure 2B, Figure 5; state
1469 flow, for substance B	1470 I_B	1471 [mol·s ⁻¹]	1472 system-related extensive quantity; 1473 Figure 7
1474 flux, for substance B	1475 J_B	1476 <i>varies</i>	1477 size-specific quantity; Figure 7
1478 inorganic phosphate	1479 P_i		1480 Figure 3
1481 intact cell number, viable cell number	1482 N_{vce}	1483 [x]	1484 Table 5; viable cells, intact of plasma 1485 membrane barrier function
1486 LEAK	1487 LEAK		1488 Table 1, Figure 5; state
1489 mass of sample X	1490 m_X	1491 [kg]	1492 Table 4
1493 mass of entity X	1494 M_X	1495 [kg]	1496 mass of object X; Table 4
1497 MITOCARTA			1498 https://www.broadinstitute.org/scientific-community/science/programs/metabolic-disease-program/publications/mitocarta/mitocarta-in-0
1499 MitoPedia			1500 http://www.bioblast.at/index.php/MitoPedia
1501 mitochondria or mitochondrial	1502 mt		1503 Box 1
1504 mitochondrial DNA	1505 mtDNA		1506 Box 1
1507 mitochondrial concentration	1508 $C_{mtE} = mtE \cdot V^{-1}$	1509 [mtEU·m ⁻³]	1510 Table 4
1511 mitochondrial content	1512 $mtE_X = mtE \cdot N_X^{-1}$	1513 [mtEU·x ⁻¹]	1514 Table 4
1515 mitochondrial elemental unit	1516 mtEU	1517 <i>varies</i>	1518 Table 4, specific units for mt-marker
1519 mitochondrial inner membrane	1520 mtIM		1521 Figure 2; MIM is widely used; the first 1522 M is replaced by mt; Box 1
1523 mitochondrial outer membrane	1524 mtOM		1525 Figure 2; MOM is widely used; the first 1526 M is replaced by mt; Box 1
1527 mitochondrial recovery	1528 Y_{mtE}		1529 fraction of <i>mtE</i> recovered in sample 1530 from the tissue of origin
1531 mitochondrial yield	1532 $Y_{mtE/m}$		1533 $Y_{mtE/m} = Y_{mtE} \cdot D_{mtE}$
1534 negative	1535 neg		1536 Figure 3
1537 number concentration of X	1538 C_{NX}	1539 [x·m ⁻³]	1540 Table 4
1541 number of entities X	1542 N_X	1543 [x]	1544 Table 4, Figure 7
1545 number of entity B	1546 N_B	1547 [x]	1548 Table 4
1549 oxidative phosphorylation	1550 OXPHOS		1551 Table 1, Figure 5; state
1552 oxygen concentration	1553 $c_{O_2} = n_{O_2} \cdot V^{-1}$; [O ₂]	1554 [mol·m ⁻³]	1555 Section 3.2
1556 oxygen flux, in reaction r	1557 J_{rO_2}	1558 <i>varies</i>	1559 Figure 1
1560 permeabilized cell number	1561 N_{pce}	1562 [x]	1563 Table 5; experimental permeabilization 1564 of plasma membrane; $N_{\text{pce}} = N_{\text{cell}}$
1565 phosphorylation of ADP to ATP	1566 P_{\gg}		1567 Section 2.2

1476	positive	pos	Figure 3
1477	proton in the negative compartment	H^+_{neg}	Figure 3
1478	proton in the positive compartment	H^+_{pos}	Figure 3
1479	rate of electron transfer in ET state	E	ET-capacity; Table 1
1480	rate of LEAK respiration	L	Table 1
1481	rate of oxidative phosphorylation	P	OXPPOS capacity; Table 1
1482	rate of residual oxygen consumption	ROx	Table 1, Figure 1
1483	residual oxygen consumption	ROX	Table 1; state
1484	respiratory supercomplex	SC I _n III _n IV _n	Box 1; supramolecular assemblies composed of variable copy numbers (n) of CI, CIII and CIV
1485			
1486			
1487	specific mitochondrial density	$D_{mtE} = mtE \cdot m_X^{-1}$	[mtEU·kg ⁻¹] Table 4
1488	volume	V	[m ⁻³] Table 7
1489	weight, dry weight	W_d	[kg] used as mass of sample X ; Figure 7
1490	weight, wet weight	W_w	[kg] used as mass of sample X ; Figure 7
1491			

1492

1493

1494 Acknowledgements

1495 We thank M. Beno for management assistance. This publication is based upon work from COST
 1496 Action CA15203 MitoEAGLE, supported by COST (European Cooperation in Science and
 1497 Technology), and K-Regio project MitoFit (E.G.).

1498

1499 **Competing financial interests:** E.G. is founder and CEO of Oroboros Instruments, Innsbruck,
 1500 Austria.

1501

1502

1503 5. References

1504

- 1505 Altmann R (1894) Die Elementarorganismen und ihre Beziehungen zu den Zellen. Zweite vermehrte Auflage.
 1506 Verlag Von Veit & Comp, Leipzig:160 pp.
- 1507 Beard DA (2005) A biophysical model of the mitochondrial respiratory system and oxidative phosphorylation.
 1508 PLoS Comput Biol 1(4):e36.
- 1509 Benda C (1898) Weitere Mitteilungen über die Mitochondria. Verh Dtsch Physiol Ges:376-83.
- 1510 Birkedal R, Laasmaa M, Vendelin M (2014) The location of energetic compartments affects energetic
 1511 communication in cardiomyocytes. Front Physiol 5:376.
- 1512 Breton S, Beaupré HD, Stewart DT, Hoeh WR, Blier PU (2007) The unusual system of doubly uniparental
 1513 inheritance of mtDNA: isn't one enough? Trends Genet 23:465-74.
- 1514 Brown GC (1992) Control of respiration and ATP synthesis in mammalian mitochondria and cells. Biochem J
 1515 284:1-13.
- 1516 Calvo SE, Klauser CR, Mootha VK (2016) MitoCarta2.0: an updated inventory of mammalian mitochondrial
 1517 proteins. Nucleic Acids Research 44:D1251-7.
- 1518 Calvo SE, Julien O, Clauser KR, Shen H, Kamer KJ, Wells JA, Mootha VK (2017) Comparative analysis of
 1519 mitochondrial N-termini from mouse, human, and yeast. Mol Cell Proteomics 16:512-23.
- 1520 Campos JC, Queliconi BB, Bozi LHM, Bechara LRG, Dourado PMM, Andres AM, Jannig PR, Gomes KMS,
 1521 Zambelli VO, Rocha-Resende C, Guatimosim S, Brum PC, Mochly-Rosen D, Gottlieb RA, Kowaltowski AJ,
 1522 Ferreira JCB (2017) Exercise reestablishes autophagic flux and mitochondrial quality control in heart failure.
 1523 Autophagy 13:1304-317.
- 1524 Canton M, Luvisetto S, Schmehl I, Azzone GF (1995) The nature of mitochondrial respiration and
 1525 discrimination between membrane and pump properties. Biochem J 310:477-81.
- 1526 Chance B, Williams GR (1955a) Respiratory enzymes in oxidative phosphorylation. I. Kinetics of oxygen
 1527 utilization. J Biol Chem 217:383-93.
- 1528 Chance B, Williams GR (1955b) Respiratory enzymes in oxidative phosphorylation: III. The steady state. J Biol
 1529 Chem 217:409-27.
- 1530 Chance B, Williams GR (1955c) Respiratory enzymes in oxidative phosphorylation. IV. The respiratory chain. J
 1531 Biol Chem 217:429-38.
- 1532 Chance B, Williams GR (1956) The respiratory chain and oxidative phosphorylation. Adv Enzymol Relat Subj
 1533 Biochem 17:65-134.

- 1534 Cobb LJ, Lee C, Xiao J, Yen K, Wong RG, Nakamura HK, Mehta HH, Gao Q, Ashur C, Huffman DM, Wan J,
 1535 Muzumdar R, Barzilai N, Cohen P (2016) Naturally occurring mitochondrial-derived peptides are age-
 1536 dependent regulators of apoptosis, insulin sensitivity, and inflammatory markers. *Aging (Albany NY)* 8:796-
 1537 809.
- 1538 Cohen ER, Cvitas T, Frey JG, Holmström B, Kuchitsu K, Marquardt R, Mills I, Pavese F, Quack M, Stohner J,
 1539 Strauss HL, Takami M, Thor HL (2008) Quantities, units and symbols in physical chemistry, IUPAC Green
 1540 Book, 3rd Edition, 2nd Printing, IUPAC & RSC Publishing, Cambridge.
- 1541 Cooper H, Hedges LV, Valentine JC, eds (2009) *The handbook of research synthesis and meta-analysis*. Russell
 1542 Sage Foundation.
- 1543 Coopersmith J (2010) *Energy, the subtle concept. The discovery of Feynman's blocks from Leibnitz to Einstein*.
 1544 Oxford University Press:400 pp.
- 1545 Cummins J (1998) Mitochondrial DNA in mammalian reproduction. *Rev Reprod* 3:172-82.
- 1546 Dai Q, Shah AA, Garde RV, Yonish BA, Zhang L, Medvitz NA, Miller SE, Hansen EL, Dunn CN, Price TM
 1547 (2013) A truncated progesterone receptor (PR-M) localizes to the mitochondrion and controls cellular
 1548 respiration. *Mol Endocrinol* 27:741-53.
- 1549 Divakaruni AS, Brand MD (2011) The regulation and physiology of mitochondrial proton leak. *Physiology*
 1550 (Bethesda) 26:192-205.
- 1551 Doerrier C, Garcia-Souza LF, Krumschnabel G, Wohlfarter Y, Mészáros AT, Gnaiger E (2018) High-Resolution
 1552 Fluorescence Respirometry and OXPHOS protocols for human cells, permeabilized fibres from small biopsies of
 1553 muscle and isolated mitochondria. *Methods Mol. Biol.* (in press)
- 1554 Doskey CM, van 't Erve TJ, Wagner BA, Buettner GR (2015) Moles of a substance per cell is a highly
 1555 informative dosing metric in cell culture. *PLOS ONE* 10:e0132572.
- 1556 Drahotová Z, Milerová M, Stieglerová A, Houstek J, Ostádal B (2004) Developmental changes of cytochrome *c*
 1557 oxidase and citrate synthase in rat heart homogenate. *Physiol Res* 53:119-22.
- 1558 Duarte FV, Palmeira CM, Rolo AP (2014) The role of microRNAs in mitochondria: small players acting wide.
 1559 *Genes (Basel)* 5:865-86.
- 1560 Ernster L, Schatz G (1981) Mitochondria: a historical review. *J Cell Biol* 91:227s-55s.
- 1561 Estabrook RW (1967) Mitochondrial respiratory control and the polarographic measurement of ADP:O ratios.
 1562 *Methods Enzymol* 10:41-7.
- 1563 Faber C, Zhu ZJ, Castellino S, Wagner DS, Brown RH, Peterson RA, Gates L, Barton J, Bickett M, Hagerty L,
 1564 Kimbrough C, Sola M, Bailey D, Jordan H, Elangbam CS (2014) Cardiolipin profiles as a potential
 1565 biomarker of mitochondrial health in diet-induced obese mice subjected to exercise, diet-restriction and
 1566 ephedrine treatment. *J Appl Toxicol* 34:1122-9.
- 1567 Fell D (1997) *Understanding the control of metabolism*. Portland Press.
- 1568 Garlid KD, Beavis AD, Ratkje SK (1989) On the nature of ion leaks in energy-transducing membranes. *Biochim*
 1569 *Biophys Acta* 976:109-20.
- 1570 Garlid KD, Semrad C, Zinchenko V. Does redox slip contribute significantly to mitochondrial respiration? In:
 1571 Schuster S, Rigoulet M, Ouhabi R, Mazat J-P, eds (1993) *Modern trends in biothermokinetics*. Plenum Press,
 1572 New York, London:287-93.
- 1573 Gerö D, Szabo C (2016) Glucocorticoids suppress mitochondrial oxidant production via upregulation of
 1574 uncoupling protein 2 in hyperglycemic endothelial cells. *PLoS One* 11:e0154813.
- 1575 Gnaiger E. Efficiency and power strategies under hypoxia. Is low efficiency at high glycolytic ATP production a
 1576 paradox? In: *Surviving Hypoxia: Mechanisms of Control and Adaptation*. Hochachka PW, Lutz PL, Sick T,
 1577 Rosenthal M, Van den Thillart G, eds (1993a) CRC Press, Boca Raton, Ann Arbor, London, Tokyo:77-109.
- 1578 Gnaiger E (1993b) Nonequilibrium thermodynamics of energy transformations. *Pure Appl Chem* 65:1983-2002.
- 1579 Gnaiger E (2001) Bioenergetics at low oxygen: dependence of respiration and phosphorylation on oxygen and
 1580 adenosine diphosphate supply. *Respir Physiol* 128:277-97.
- 1581 Gnaiger E (2009) Capacity of oxidative phosphorylation in human skeletal muscle. *New perspectives of*
 1582 *mitochondrial physiology*. *Int J Biochem Cell Biol* 41:1837-45.
- 1583 Gnaiger E (2014) *Mitochondrial pathways and respiratory control. An introduction to OXPHOS analysis*. 4th ed.
 1584 *Mitochondr Physiol Network* 19.12. Oroboros MiPNet Publications, Innsbruck:80 pp.
- 1585 Gnaiger E, Méndez G, Hand SC (2000) High phosphorylation efficiency and depression of uncoupled respiration
 1586 in mitochondria under hypoxia. *Proc Natl Acad Sci USA* 97:11080-5.
- 1587 Greggio C, Jha P, Kulkarni SS, Lagarrigue S, Broskey NT, Boutant M, Wang X, Conde Alonso S, Ofori E,
 1588 Auwerx J, Cantó C, Amati F (2017) Enhanced respiratory chain supercomplex formation in response to
 1589 exercise in human skeletal muscle. *Cell Metab* 25:301-11.
- 1590 Hinkle PC (2005) P/O ratios of mitochondrial oxidative phosphorylation. *Biochim Biophys Acta* 1706:1-11.
- 1591 Hofstadter DR (1979) Gödel, Escher, Bach: An eternal golden braid. A metaphorical fugue on minds and
 1592 machines in the spirit of Lewis Carroll. Harvester Press:499 pp.
- 1593 Illaste A, Laasmaa M, Peterson P, Vendelin M (2012) Analysis of molecular movement reveals latticelike
 1594 obstructions to diffusion in heart muscle cells. *Biophys J* 102:739-48.
- 1595 Jasienski M, Bazzaz FA (1999) The fallacy of ratios and the testability of models in biology. *Oikos* 84:321-26.

- 1596 Jephthina N, Beraud N, Sepp M, Birkedal R, Vendelin M (2011) Permeabilized rat cardiomyocyte response
1597 demonstrates intracellular origin of diffusion obstacles. *Biophys J* 101:2112-21.
- 1598 Klepinin A, Ounpuu L, Guzun R, Chekulayev V, Timohhina N, Tepp K, Shevchuk I, Schlattner U, Kaambre T
1599 (2016) Simple oxygraphic analysis for the presence of adenylate kinase 1 and 2 in normal and tumor cells. *J*
1600 *Bioenerg Biomembr* 48:531-48.
- 1601 Klingenberg M (2017) UCP1 - A sophisticated energy valve. *Biochimie* 134:19-27.
- 1602 Koit A, Shevchuk I, Ounpuu L, Klepinin A, Chekulayev V, Timohhina N, Tepp K, Puurand M, Truu L, Heck K,
1603 Valvere V, Guzun R, Kaambre T (2017) Mitochondrial respiration in human colorectal and breast cancer
1604 clinical material is regulated differently. *Oxid Med Cell Longev* 1372640.
- 1605 Komlódi T, Tretter L (2017) Methylene blue stimulates substrate-level phosphorylation catalysed by succinyl-
1606 CoA ligase in the citric acid cycle. *Neuropharmacology* 123:287-98.
- 1607 Lane N (2005) Power, sex, suicide: mitochondria and the meaning of life. Oxford University Press:354 pp.
- 1608 Larsen S, Nielsen J, Neigaard Nielsen C, Nielsen LB, Wibrand F, Stride N, Schroder HD, Boushel RC, Helge
1609 JW, Dela F, Hey-Mogensen M (2012) Biomarkers of mitochondrial content in skeletal muscle of healthy
1610 young human subjects. *J Physiol* 590:3349-60.
- 1611 Lee C, Zeng J, Drew BG, Sallam T, Martin-Montalvo A, Wan J, Kim SJ, Mehta H, Hevener AL, de Cabo R,
1612 Cohen P (2015) The mitochondrial-derived peptide MOTS-c promotes metabolic homeostasis and reduces
1613 obesity and insulin resistance. *Cell Metab* 21:443-54.
- 1614 Lee SR, Kim HK, Song IS, Youm J, Dizon LA, Jeong SH, Ko TH, Heo HJ, Ko KS, Rhee BD, Kim N, Han J
1615 (2013) Glucocorticoids and their receptors: insights into specific roles in mitochondria. *Prog Biophys Mol*
1616 *Biol* 112:44-54.
- 1617 Leek BT, Mudaliar SR, Henry R, Mathieu-Costello O, Richardson RS (2001) Effect of acute exercise on citrate
1618 synthase activity in untrained and trained human skeletal muscle. *Am J Physiol Regul Integr Comp Physiol*
1619 280:R441-7.
- 1620 Lemieux H, Blier PU, Gnaiger E (2017) Remodeling pathway control of mitochondrial respiratory capacity by
1621 temperature in mouse heart: electron flow through the Q-junction in permeabilized fibers. *Sci Rep* 7:2840.
- 1622 Lenaz G, Tioli G, Falasca AI, Genova ML (2017) Respiratory supercomplexes in mitochondria. In: *Mechanisms*
1623 *of primary energy trasduction in biology*. M Wikstrom (ed) Royal Society of Chemistry Publishing, London,
1624 UK:296-337.
- 1625 Margulis L (1970) Origin of eukaryotic cells. New Haven: Yale University Press.
- 1626 Meinild Lundby AK, Jacobs RA, Gehrig S, de Leur J, Hauser M, Bonne TC, Flück D, Dandanell S, Kirk N,
1627 Kaech A, Ziegler U, Larsen S, Lundby C (2018) Exercise training increases skeletal muscle mitochondrial
1628 volume density by enlargement of existing mitochondria and not de novo biogenesis. *Acta Physiol* 222,
1629 e12905.
- 1630 Menshikova EV, Ritov VB, Fairfull L, Ferrell RE, Kelley DE, Goodpaster BH (2006) Effects of exercise on
1631 mitochondrial content and function in aging human skeletal muscle. *J Gerontol A Biol Sci Med Sci* 61:534-
1632 40.
- 1633 Menshikova EV, Ritov VB, Ferrell RE, Azuma K, Goodpaster BH, Kelley DE (2007) Characteristics of skeletal
1634 muscle mitochondrial biogenesis induced by moderate-intensity exercise and weight loss in obesity. *J Appl*
1635 *Physiol* (1985) 103:21-7.
- 1636 Menshikova EV, Ritov VB, Toledo FG, Ferrell RE, Goodpaster BH, Kelley DE (2005) Effects of weight loss
1637 and physical activity on skeletal muscle mitochondrial function in obesity. *Am J Physiol Endocrinol Metab*
1638 288:E818-25.
- 1639 Miller GA (1991) The science of words. Scientific American Library New York:276 pp.
- 1640 Mitchell P (1961) Coupling of phosphorylation to electron and hydrogen transfer by a chemi-osmotic type of
1641 mechanism. *Nature* 191:144-8.
- 1642 Mitchell P (2011) Chemiosmotic coupling in oxidative and photosynthetic phosphorylation. *Biochim Biophys*
1643 *Acta Bioenergetics* 1807:1507-38.
- 1644 Mogensen M, Sahlin K, Fernström M, Glintborg D, Vind BF, Beck-Nielsen H, Højlund K (2007) Mitochondrial
1645 respiration is decreased in skeletal muscle of patients with type 2 diabetes. *Diabetes* 56:1592-9.
- 1646 Mohr PJ, Phillips WD (2015) Dimensionless units in the SI. *Metrologia* 52:40-7.
- 1647 Moreno M, Giacco A, Di Munno C, Goglia F (2017) Direct and rapid effects of 3,5-diiodo-L-thyronine (T2).
1648 *Mol Cell Endocrinol* 7207:30092-8.
- 1649 Morrow RM, Picard M, Derbeneva O, Leipzig J, McManus MJ, Gousspillou G, Barbat-Artigas S, Dos Santos C,
1650 Hepple RT, Murdock DG, Wallace DC (2017) Mitochondrial energy deficiency leads to hyperproliferation of
1651 skeletal muscle mitochondria and enhanced insulin sensitivity. *Proc Natl Acad Sci U S A* 114:2705-10.
- 1652 Murley A, Nunnari J (2016) The emerging network of mitochondria-organelle contacts. *Mol Cell* 61:648-53.
- 1653 National Academies of Sciences, Engineering, and Medicine (2018) International coordination for science data
1654 infrastructure: Proceedings of a workshop—in brief. Washington, DC: The National Academies Press. doi:
1655 <https://doi.org/10.17226/25015>.
- 1656 Palmfeldt J, Bross P (2017) Proteomics of human mitochondria. *Mitochondrion* 33:2-14.

- 1657 Paradies G, Paradies V, De Benedictis V, Ruggiero FM, Petrosillo G (2014) Functional role of cardiolipin in
1658 mitochondrial bioenergetics. *Biochim Biophys Acta* 1837:408-17.
- 1659 Pesta D, Gnaiger E (2012) High-Resolution Respirometry. *OXPHOS protocols for human cells and*
1660 *permeabilized fibres from small biopsies of human muscle. Methods Mol Biol* 810:25-58.
- 1661 Pesta D, Hoppel F, Macek C, Messner H, Faulhaber M, Kobel C, Parson W, Burtscher M, Schocke M, Gnaiger
1662 E (2011) Similar qualitative and quantitative changes of mitochondrial respiration following strength and
1663 endurance training in normoxia and hypoxia in sedentary humans. *Am J Physiol Regul Integr Comp Physiol*
1664 301:R1078–87.
- 1665 Price TM, Dai Q (2015) The role of a mitochondrial progesterone receptor (PR-M) in progesterone action.
1666 *Semin Reprod Med* 33:185-94.
- 1667 Puchowicz MA, Varnes ME, Cohen BH, Friedman NR, Kerr DS, Hoppel CL (2004) Oxidative phosphorylation
1668 analysis: assessing the integrated functional activity of human skeletal muscle mitochondria – case studies.
1669 *Mitochondrion* 4:377-85. Puntschart A, Claassen H, Jostardt K, Hoppeler H, Billeter R (1995) mRNAs of
1670 enzymes involved in energy metabolism and mtDNA are increased in endurance-trained athletes. *Am J*
1671 *Physiol* 269:C619-25.
- 1672 Quiros PM, Mottis A, Auwerx J (2016) Mitonuclear communication in homeostasis and stress. *Nat Rev Mol*
1673 *Cell Biol* 17:213-26.
- 1674 Rackham O, Mercer TR, Filipovska A (2012) The human mitochondrial transcriptome and the RNA-binding
1675 proteins that regulate its expression. *WIREs RNA* 3:675–95.
- 1676 Reichmann H, Hoppeler H, Mathieu-Costello O, von Bergen F, Pette D (1985) Biochemical and ultrastructural
1677 changes of skeletal muscle mitochondria after chronic electrical stimulation in rabbits. *Pflugers Arch* 404:1-
1678 9.
- 1679 Renner K, Amberger A, Konwalinka G, Gnaiger E (2003) Changes of mitochondrial respiration, mitochondrial
1680 content and cell size after induction of apoptosis in leukemia cells. *Biochim Biophys Acta* 1642:115-23.
- 1681 Rich P (2003) Chemiosmotic coupling: The cost of living. *Nature* 421:583.
- 1682 Rostovtseva TK, Sheldon KL, Hassanzadeh E, Monge C, Saks V, Bezrukov SM, Sackett DL (2008) Tubulin
1683 binding blocks mitochondrial voltage-dependent anion channel and regulates respiration. *Proc Natl Acad Sci*
1684 *USA* 105:18746-51.
- 1685 Rustin P, Parfait B, Chretien D, Bourgeron T, Djouadi F, Bastin J, Rötig A, Munnich A (1996) Fluxes of
1686 nicotinamide adenine dinucleotides through mitochondrial membranes in human cultured cells. *J Biol Chem*
1687 271:14785-90.
- 1688 Saks VA, Veksler VI, Kuznetsov AV, Kay L, Sikk P, Tiivel T, Tranqui L, Olivares J, Winkler K, Wiedemann F,
1689 Kunz WS (1998) Permeabilised cell and skinned fiber techniques in studies of mitochondrial function in
1690 vivo. *Mol Cell Biochem* 184:81-100.
- 1691 Salabei JK, Gibb AA, Hill BG (2014) Comprehensive measurement of respiratory activity in permeabilized cells
1692 using extracellular flux analysis. *Nat Protoc* 9:421-38.
- 1693 Sazanov LA (2015) A giant molecular proton pump: structure and mechanism of respiratory complex I. *Nat Rev*
1694 *Mol Cell Biol* 16:375-88.
- 1695 Schneider TD (2006) Claude Shannon: biologist. The founder of information theory used biology to formulate
1696 the channel capacity. *IEEE Eng Med Biol Mag* 25:30-3.
- 1697 Schönfeld P, Dymkowska D, Wojtczak L (2009) Acyl-CoA-induced generation of reactive oxygen species in
1698 mitochondrial preparations is due to the presence of peroxisomes. *Free Radic Biol Med* 47:503-9.
- 1699 Schultz J, Wiesner RJ (2000) Proliferation of mitochondria in chronically stimulated rabbit skeletal muscle--
1700 transcription of mitochondrial genes and copy number of mitochondrial DNA. *J Bioenerg Biomembr* 32:627-
1701 34.
- 1702 Speijer D (2016) Being right on Q: shaping eukaryotic evolution. *Biochem J* 473:4103-27.
- 1703 Sugiura A, Mattie S, Prudent J, McBride HM (2017) Newly born peroxisomes are a hybrid of mitochondrial and
1704 ER-derived pre-peroxisomes. *Nature* 542:251-4.
- 1705 Simson P, Jephthina N, Laasmaa M, Peterson P, Birkedal R, Vendelin M (2016) Restricted ADP movement in
1706 cardiomyocytes: Cytosolic diffusion obstacles are complemented with a small number of open mitochondrial
1707 voltage-dependent anion channels. *J Mol Cell Cardiol* 97:197-203.
- 1708 Stucki JW, Ineichen EA (1974) Energy dissipation by calcium recycling and the efficiency of calcium transport
1709 in rat-liver mitochondria. *Eur J Biochem* 48:365-75.
- 1710 Tonkonogi M, Harris B, Sahlin K (1997) Increased activity of citrate synthase in human skeletal muscle after a
1711 single bout of prolonged exercise. *Acta Physiol Scand* 161:435-6.
- 1712 Torralba D, Baixauli F, Sánchez-Madrid F (2016) Mitochondria know no boundaries: mechanisms and functions
1713 of intercellular mitochondrial transfer. *Front Cell Dev Biol* 4:107. eCollection 2016.
- 1714 Vamecq J, Schepers L, Parmentier G, Mannaerts GP (1987) Inhibition of peroxisomal fatty acyl-CoA oxidase by
1715 antimycin A. *Biochem J* 248:603-7.
- 1716 Waczulikova I, Habodaszova D, Cagalinec M, Ferko M, Ulicna O, Mateasik A, Sikurova L, Ziegelhöffer A
1717 (2007) Mitochondrial membrane fluidity, potential, and calcium transients in the myocardium from acute
1718 diabetic rats. *Can J Physiol Pharmacol* 85:372-81.

- 1719 Wagner BA, Venkataraman S, Buettner GR (2011) The rate of oxygen utilization by cells. *Free Radic Biol Med*
1720 51:700-712.
- 1721 Wang H, Hiatt WR, Barstow TJ, Brass EP (1999) Relationships between muscle mitochondrial DNA content,
1722 mitochondrial enzyme activity and oxidative capacity in man: alterations with disease. *Eur J Appl Physiol*
1723 *Occup Physiol* 80:22-7.
- 1724 Watt IN, Montgomery MG, Runswick MJ, Leslie AG, Walker JE (2010) Bioenergetic cost of making an
1725 adenosine triphosphate molecule in animal mitochondria. *Proc Natl Acad Sci U S A* 107:16823-7.
- 1726 Weibel ER, Hoppeler H (2005) Exercise-induced maximal metabolic rate scales with muscle aerobic capacity. *J*
1727 *Exp Biol* 208:1635-44.
- 1728 White DJ, Wolff JN, Pierson M, Gemmell NJ (2008) Revealing the hidden complexities of mtDNA inheritance.
1729 *Mol Ecol* 17:4925-42.
- 1730 Wikström M, Hummer G (2012) Stoichiometry of proton translocation by respiratory complex I and its
1731 mechanistic implications. *Proc Natl Acad Sci U S A* 109:4431-6.
- 1732 Williams EG, Wu Y, Jha P, Dubuis S, Blattmann P, Argmann CA, Houten SM, Amariuta T, Wolski W,
1733 Zamboni N, Aebersold R, Auwerx J (2016) Systems proteomics of liver mitochondria function. *Science* 352
1734 (6291):aad0189
- 1735 Willis WT, Jackman MR, Messer JI, Kuzmiak-Glancy S, Glancy B (2016) A simple hydraulic analog model of
1736 oxidative phosphorylation. *Med Sci Sports Exerc* 48:990-1000.
- 1737